Mixed layer depth dominates over upwelling in regulating the seasonality of ecosystem functioning in the Peruvian Upwelling System

Tianfei Xue[1], Ivy Frenger[1], A.E. Friederike Prowe[1], Yonss Saranga José[1], and Andreas Oschlies[1,2]

[1]GEOMAR Helmholtz Centre for Ocean Research Kiel, Kiel, Germany
[2]Christian-Albrechts-University Kiel, Germany

Correspondence: Tianfei Xue (txue@geomar.de)

Abstract. The Peruvian Upwelling System hosts ~~an extremely high productive marine ecosystem~~ a marine ecosystem with extremely high productivity. Observations show that the Peruvian Upwelling System is the only Eastern Boundary Upwelling ~~Systems~~ System (EBUS) with an out-of-phase relationship ~~of~~ between seasonal surface chlorophyll concentrations and upwelling intensity. This "seasonal paradox" triggers the following questions: (1) ~~what is the uniqueness~~ What are the unique characteristics of the Peruvian Upwelling System, compared with other EBUS~~that leads to the out of phase relationship;~~ , that lead to the out-of-phase relationship; and (2) ~~how does this uniqueness lead to low phytoplankton biomass in austral winter despite strong upwelling and ample nutrients~~How does the seasonal paradox influence ecosystem functioning? Using observational climatologies for four EBUS, we diagnose that the Peruvian Upwelling System is ~~unique in~~ the only one to reveal that intense upwelling coincides with deep mixed layers. We then apply a coupled regional ocean circulation-biogeochemical model (CROCO-BioEBUS) to assess how the interplay between mixed ~~layer and upwelling is regulating~~ layers and upwelling regulates the seasonality of surface chlorophyll in the Peruvian Upwelling System. ~~The model recreates~~ Our model reproduces the "seasonal paradox" within 200 km off the Peruvian coast. We confirm previous findings ~~that deep mixed layers, which~~ regarding the main contribution of mixed layer depth to the seasonality of chlorophyll, relative to upwelling. Deep mixed layers in austral winter cause vertical dilution ~~and stronger~~ of phytoplankton and strong light limitation, ~~mostly drive the diametrical seasonality of chlorophyll relative to upwelling. In contrast to previous studies, reduced phytoplankton growth due to enhanced upwelling of cold waters and lateral advection are~~ impacting growth. The effect of advection on the buildup of phytoplankton biomass, though second-order~~drivers of low surface chlorophyll concentrations~~, is consistent with previous findings for the Peruvian system and other EBUS, with enhanced offshore export opposing the coastal buildup of biomass. In addition, we find that the relatively colder temperatures of upwelled waters slightly dampen phytoplankton productivity and further slow the buildup of phytoplankton biomass. This impact from the combination of deep mixed layers and upwelling propagates ~~up~~ through the ecosystem, from primary production to export and export efficiency. Our findings ~~emphasize~~ emphasise the crucial role of the interplay ~~of the mixed layer~~ between mixed layer depth and upwelling and suggest that surface chlorophyll may increase, along with a weakened seasonal paradox, in response to shoaling mixed layers under climate change.

Copyright statement.

1 Introduction

The Peruvian Upwelling System (PUS) hosts a disproportionally productive ecosystem~~and supports~~ , supporting 10% of the world's fishing yield while covering only 0.1% of the ocean area (Chavez et al., 2008). As one of the Eastern Boundary Upwelling Systems (EBUS), ~~upwelling-favorable winds bring up~~ winds favouring upwelling raise cool, nutrient-rich waters to the surface, supporting high primary production and fish yield. ~~At the same time, the~~ Simultaneously, high primary production, together with subsequent export and ~~remineralization in part causes~~ remineralisation contributes to the formation of a subsurface ~~oxygen deficient~~ oxygen-deficient zone which is particularly shallow and intense in the PUS (Fuenzalida et al., 2009; Stramma et al., 2010; Getzlaff et al., 2016). Particularly ~~via~~ due to its high productivity, the response of the PUS to climate change is of great social and economic interest (Pauly et al., 1998; Bakun, 1990; Bakun et al., 2010), and a variety of studies have investigated how physical and biogeochemical processes influence the production of phytoplankton ~~and~~ as well as its potential links to ecosystem functioning in the PUS.

While the PUS has been frequently compared to other EBUS (e.g., the Benguela, California, and Canary Systems), it is set apart by how ~~the~~ surface chlorophyll responds to the variation of upwelling on a seasonal scale. The high productivity of EBUS primarily benefits from the upwelling of nutrient-rich waters, driven by ~~the~~ alongshore equatorward winds. Hence, it is commonly assumed that the magnitude of phytoplankton biomass in EBUS is directly correlated with the wind-driven upwelling intensity (Bakun, 1973). However, in the PUS, upwelling intensity and surface chlorophyll are not correlated on ~~the seasonal scale (hereafter referred to as "seasonal paradox"; Chavez and Messié, 2009). Indeed~~a seasonal scale (hereafter referred to as "seasonal paradox"; Chavez, 1995; Thomas et al., 2001; Echevin et al., 2008; Chavez and Messié, 2009) . Instead, they are out of phase, with the lowest surface chlorophyll concentration in austral winter ~~when upwelling intensity is highest~~ corresponding to maximum upwelling intensity (Calienes et al., 1985). Echevin et al. (2008) ~~and Messié and Chavez (2015) argue that mixed layers are deep when upwelling and nutrient supply is highest. Deep mixed layers would cause dilution of phytoplankton, and growth to be limited by~~ used a regional coupled physical-biogeochemical model to simulate the "seasonal paradox" and found that deep mixed layers caused dilution of surface phytoplankton, reduced growth due to limited light, and subsequently ~~iron~~ reduced iron levels (as phytoplankton ~~needs~~ require more iron under ~~low light condition), leading~~ low-light conditions). This ultimately leads to low chlorophyll under strong upwelling conditions. ~~Lower surface radiation~~ Results from Messié and Chavez (2015) corroborated iron and light limitations found in Echevin et al. (2008), showing additionally that relatively strong offshore advection in austral winter regulated the buildup of phytoplankton and thus also contributed to the seasonal paradox. Guillen and Calienes (1981) suggested that lower surface irradiation in winter might amplify light limitation ~~(Guillen and Calienes, 1981). Hence, while upwelling and mixed layer depth both regulate phytoplankton , the interplay of the two has not been assessed. Further, it remains unclear~~ and further limit phytoplankton growth, while insolation was found not to play a major role in Echevin et al. (2008). Additionally, Echevin et al. (2008) concluded that temperature played no role in regulating phytoplankton growth. Despite previous research on surface chlorophyll seasonality, uncertainty still remains

regarding why the seasonal paradox occurs only in the PUS and not in the other EBUS, and it is unexplored how the seasonal paradox affects ecosystem functioning.

~~To this end, this study will address~~ This study addresses the following key questions: (1) what ~~is the uniqueness of PUS~~ are the unique characteristics of the PUS, compared to other EBUS~~that leads to the~~ , that lead to this seasonal paradox; (2) ~~how does the unique mechanism limit phytoplankton from growing under strong upwelling~~what are the mechanisms that cause low surface phytoplankton in winter; and (3) how ~~will this further~~ do these mechanisms affect ecosystem functioning.

2 Data and Methods

2.1 Regional ocean circulation-biogeochemical model: ~~set up~~ setup and simulation

We use a climatological simulation of the three-dimensional regional ocean circulation model CROCO (Coastal and Regional Ocean COmmunity model; Debreu et al., 2012) coupled with the biogeochemical model BioEBUS (Biogeochemical model for the Eastern Boundary Upwelling Systems; Gutknecht et al., 2013) for this study.

~~We use the same technical set-up~~ The same technical setup, including the model grid, is used as in José et al. (2017), along with an updated version of the ocean circulation model CROCO. CROCO is the next generation of the ROMS AGRIF model (Tedesco et al., 2019), and is a free-surface and split-explicit regional ocean model system (ROMS; Shchepetkin and McWilliams, 2005). We employ a two-way nesting approach, with the larger coarser-resolution domain covering the Southeast Pacific and the smaller higher-resolution domain focusing on the PUS. The larger domain has a 1/4° resolution, spanning from 69°W to 120°W and from 18°N to 40°S. The embedded "child" domain has a resolution of 1/12° and extends from 5°N to 31°S and from 69°W to 102°W (Fig. A1) ~~which~~ and is used in this study. Both ~~coarse~~ the coarse- and fine-resolution domains use 32 sigma levels in the vertical direction, with finer resolution towards the surface and shallower regions. The surface layer thickness ~~is ranging~~ ranges from 0.5 m in the coastal region (water depth around 50 m) to around 3 m in the offshore region~~(water depth~~ , corresponding to a water depth of more than 4000 m~~)~~. Initial and boundary conditions are provided by the monthly climatological SODA reanalysis (Simple Ocean Data Assimilation; Carton and Giese, 2008) from 1990−2010. ~~The surface~~ Surface forcing is based on the monthly climatological heat and freshwater fluxes from COADS (Comprehensive Ocean-Atmosphere Data Set; Worley et al., 2005), along with wind data from QuikSCAT (Quick Scatterometer; Liu et al., 1998). The physical setup is the same as in José et al. (2017) and has been evaluated therein~~. The model simulates eddy kinetic energy, sea surface height and alongshore current well, with an underestimation of the intensity of the Equator–Peru coastal current and Peru–Chile undercurrent~~, showing that the model reproduces the circulation of the region reasonably well.

The biogeochemical BioEBUS model used in this study was developed explicitly for applications to EBUS and oxygen minimum zones (Gutknecht et al., 2013). BioEBUS is a nitrogen-based model, originating from the $N_2P_2Z_2D_2$ model by Koné et al. (2005). It simulates two phytoplankton and two zooplankton groups: small and large phytoplankton, along with micro- and mesozooplankton. ~~Further~~Furthermore, there are two detritus pools~~categorized based on~~ , categorised by size. BioEBUS resolves the N species (nitrate, nitrite and ammonium) and simulates processes under oxic, hypoxic and suboxic conditions (e.g.~~remineralization,~~ , remineralisation, nitrification, denitrification and anammox). The BioEBUS model was first used to

study the Peruvian marine biogeochemistry by Montes et al. (2014), and is capable of producing a realistic simulation of the oxygen distribution. Initial and boundary conditions for nitrate and oxygen are taken from CARS (CSIRO (Commonwealth Scientific and Industrial Research Organisation) Atlas of Regional Seas; Ridgway et al., 2002), and initial conditions for phytoplankton are based on monthly climatological SeaWiFS (Sea-viewing Wide Field-of-view Sensor; O'Reilly et al., 1998) estimates. A detailed description of these biogeochemical processes can be found in Gutknecht et al. (2013). The parameter setting is settings are the same as in José et al. (2017), with except for a few adjustments to biological parameters (Table. A1) to make the improve the fit between the simulated ecology, in particular phytoplankton and zooplankton biomass and seasonality, better fit and the observations.

CROCO-BioEBUS is run in coupled mode from the startbeginning of the simulation. The time-stepping of the physical model is the same as the coupling timestep, time step, with a duration of 1200 seconds. The time-stepping of the biogeochemical model is has a duration of 400 seconds. The coupled model is run for a 25-year spin-up period. Biogeochemical and physical fields are spun-up Physical and biogeochemical fields are spun up after one year for the upper 10 mwhile it takes longer for the deep waters (1000, while waters in the depth range of upwelling source (100 m) require 3–10 years longer to reach a statistical quasi-equilibrium (Fig. C1). In this study, we use monthly output of the final We run the model for a total of 30 climatologically-forced years, using the last five years for our analyses(years 26 – 30)the analyses. As we look at observe from the surface ecology, our results are not sensitive to the deep deep ocean spin-up. This study focuses on the 200 km band off the Peruvian coast (white line region in Fig. 1a-b)where shows the , which shows clear seasonal variation along with the as well as strong upwelling.

2.2 Analyses Analysis approaches

To assess the seasonal variance of phytoplankton biomass concentration in each grid box (C)we analyze with , we analysed the budget of the phytoplankton biomass and how its tendency is driven by physical versus biological processes:

$$\frac{\partial C}{\partial t} = PHY(C) + BIO(C) \tag{1}$$

with $[BIO = PP - GRAZ - MORT - EXU - SINK;\ PHY = MIX + ADV]$

PHY represents the physical processes, including advection and mixing. The BIO term stands for , whereas BIO represents the biological processes, namely primary production PP, consumptive mortality $GRAZ$, natural mortality , exudation and sinking. We analyse in $MORT$, exudation EXU and sinking $SINK$. All biological and physical fluxes except for entrainment were saved monthly from the simulation, with units of mmol N m^{-3} s^{-1}, and we integrated the terms offline over the mixed layer depth (MLD) using the croco-tools provided for post-processing (https://www.croco-ocean.org/download/croco-project/). We calculated the monthly entrainment as a residual, following the calculation of entrainment for physical variables in the CROCO code. That is, entrainment was calculated as the difference between the MLD-integrated biomass tendency and the sum of the biological and physical fluxes integrated over the MLD of the previous month.

We analysed in detail the drivers of PP~~: PP is~~ , which was determined by phytoplankton concentration (C) and the growth ~~rate (J)~~ factors ($L_{(PAR)}$,$L_{(T)}$,$L_{(N)}$)

$$PP = C \cdot J(N, PAR, T) L_{(PAR)} \cdot L_{(T)} \cdot L_{(N)} \tag{2}$$

where ~~the growth rate J is related to light availability for photosynthesis (PAR: photosynthetically active radiation), temperature (T) and nutrients (N: nitrate, nitrite and ammonium). The growth rate here is~~ $L_{(PAR)}$, $L_{(T)}$, $L_{(N)}$ represent the light-, temperature- or nitrogen-related growth factors, respectively. Here, the phytoplankton growth rate was defined as a multiplicative function of the light-, temperature- or nitrogen-related growth factors. ~~To quantify the~~ The limitation experienced by phytoplankton within the mixed layer L_{mld} ~~, it~~ is calculated from each growth factor ($L_{\text{(PAR)}}$, $L_{\text{(T)}}$ and $L_{\text{(N)}}$), using phytoplankton concentration (C) within the mixed layer as a weight (Eq. 3). Light-, temperature- ~~or~~ and nitrogen-related growth factors that each phytoplankton cell ~~experiences are~~ experienced were computed online.

$$L_{\text{mld}} = \frac{\sum_0^{\text{mld}} L_{\text{(PAR)}} \cdot L_{\text{(T)}} \cdot L_{\text{(N)}} \cdot C}{\sum_0^{\text{mld}} C} \tag{3}$$

For the analysis, we ~~attribute~~ attributed the seasonal change of the average phytoplankton biomass concentration (~~C_{mld}~~ΔC_{mld}) within the mixed layer to the change ~~of~~ in the integrated phytoplankton content within the mixed layer (~~B_{mld}), and the change of the~~ ΔB_{mld}), as well as the change in volume of the mixed layer (~~V_{mld}). With~~ ΔV_{mld}). Using the chain rule and the condition that $V^2 >> V\Delta V$, we ~~approximate~~ approximated a discrete change ~~of~~ in the mixed layer tracer concentration (ΔC_{mld}) ~~with~~ as follows:

$$\Delta C_{\text{mld}} = \frac{1}{V_{\text{mld}}} \Delta B_{\text{mld}} - B_{\text{mld}} \frac{\Delta V_{\text{mld}}}{V_{\text{mld}}^2} = \frac{B_{\text{mld}}}{V_{\text{mld}}} \frac{\Delta B_{\text{mld}}}{B_{\text{mld}}} - \frac{B_{\text{mld}}}{V_{\text{mld}}} \frac{\Delta V_{\text{mld}}}{V_{\text{mld}}} \tag{4}$$

To assess the relative contributions~~we then divide~~ , we then divided by $C_{\text{mld}} = B_{\text{mld}} \cdot V_{\text{mld}}^{-1}$ to obtain

$$\frac{\Delta C_{\text{mld}}}{C_{\text{mld}}} = \frac{\Delta B_{\text{mld}}}{B_{\text{mld}}} - \frac{\Delta V_{\text{mld}}}{V_{\text{mld}}} \tag{5}$$

which ~~allows attributing a decrease of~~ allowed us to attribute decreased concentration of phytoplankton in the mixed layer~~phytoplankton concentration~~ , C_{mld}, to a decrease ~~of~~ in the phytoplankton biomass B_{mld} or an increase ~~of the mixed layer~~ in the mixed-layer volume V_{mld}, and vice versa.

2.3 ~~Model~~ Observational data and model assessment

For EBUS comparisons, we digitised SeaWIFS climatological surface chlorophyll and upwelling (a combination of Ekman transport and Ekman pumping, Messié et al. (2009)), estimated based on winds from QuikSCAT, from Chavez and Messié (2009) . Additionally, we used surface nitrate data from the World Ocean Atlas (WOA; Garcia et al., 2019), the gridded ARGO mixed layer dataset (Holte et al. (2017), http://mixedlayer.ucsd.edu/), monthly climatology of MODIS sea surface temperature (SST) and chlorophyll data (https://oceancolor.gsfc.nasa.gov/data/aqua/) to analyse and evaluate the model results.

The model was ~~is~~ evaluated based on averages over the focus region~~with observational data in monthly resolution~~, with monthly observational data. The correlation coefficient between the model simulation and observations, the root mean square error (RMSE) and the ~~normalized~~ normalised standard deviation (SD) of the observations relative to the model results are shown in a Taylor diagram as a summary of the evaluation (Fig. 1c, Taylor et al. (1991); a comparison of the spatial pattern and the seasonal cycles of variables ~~are~~ is provided in the appendix, see Figs. B1-B4). Model results fit the observational data reasonably well. The model ~~performs well in simulating~~ effectively simulated sea surface temperature (SST) with R>0.95, 1<σ^*<1.2 and ~~$RMSD^*$~~ $RMSE^*$<0.4 (R: correlation coefficient, σ^*: ~~normalized~~ normalised SD, and ~~RMSD*: normalized RMSD). The model captures~~ RMSE*: normalised RMSE). It also captured the observed seasonal cycle well~~with~~ , though it produced slightly stronger seasonal variations compared to those from the observational data. ~~As for~~ Although the seasonal variation was somewhat overestimated, the simulated MLD (defined based on a 0.2 ^oC temperature difference criterion) ~~,~~ ~~though the seasonal variation is somewhat overestimated, the model simulation is~~ remained mostly within the observed range of ~~ARGO based MLD most of the time~~ ARGO-based MLD (Fig. B3). As for biogeochemical variables, the model ~~simulates surface nitratewell~~ effectively simulated surface nitrate, with R>0.95, 0.6<σ^*<1 and ~~$RMSD^*$~~ $RMSE^*$<0.4~~but overestimates~~ , but overestimated the nitrate compared to WOA. Cruise data (Fig. B2c-d) ~~shows~~ show that the overestimation could ~~arise~~ have arisen from WOA failing to capture the ~~high surface~~ high-surface nitrate concentration in the coastal region ~~with~~ under strong upwelling. A comparison of the simulated and observed seasonal cycle of surface chlorophyll in the focus region (Fig. 1d) ~~reveals~~ revealed that modelled chlorophyll generally ~~follows~~ followed the seasonal trend of satellite and *in situ* data, with the amplitude of the seasonal cycle ~~falling in between~~ in between amplitudes from satellite and *in situ* data. Overall, the model ~~shows~~ showed reasonably good agreement with observational data on a seasonal scale, sufficiently supporting an investigation of the seasonal paradox with CROCO-BioEBUS.

3 Results

3.1 Anticorrelation of chlorophyll and upwelling: The seasonal paradox only appears in the Peruvian upwelling system

Compared with other EBUS (spatial extent of EBUS regions indicated in Fig. A2), the Peruvian system is unique in that it shows a clear ~~anti-correlation~~ anticorrelation between surface chlorophyll concentration and upwelling intensity on a seasonal scale, with lowest chlorophyll concentrations when upwelling is most intense (Fig. 2a, $R^2 = 0.71$; Chavez and Messié, 2009). While the surface chlorophyll in the Benguela system does not feature a strong seasonality, surface chlorophyll closely follows upwelling intensity ~~closely~~ in the California ($R^2 = 0.92$) and Canary ($R^2 = 0.88$) systems, suggesting that upwelling of nutrient-rich waters fuels the ~~chlorophyll increase in these two systems.~~ increase in chlorophyll. Indeed, comparatively low surface nitrate concentrations indicate that nitrate is ~~used up and~~ depleted, potentially limiting phytoplankton growth throughout the year in the California system ~~, and for about~~ and for approximately half the year in the Canary system (Fig. 2b). ~~For the remainder of the year, in the Canary system enhanced surface nitrate concentrations are positively correlated with chlorophyll, suggesting that phytoplankton is stimulated by enhanced nitrate availability.~~ In contrast, the Benguela ($R^2 = 0.63$) and the

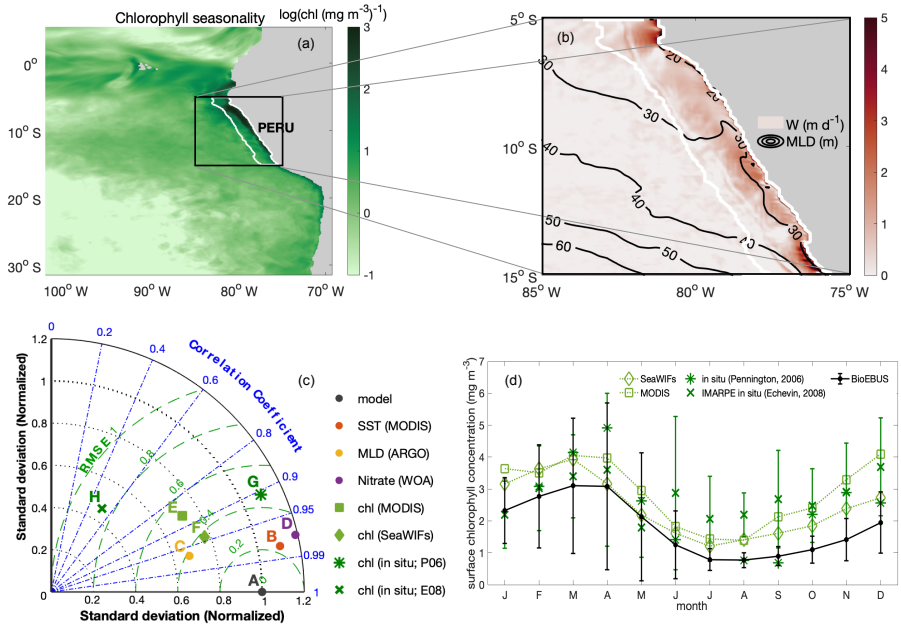

Figure 1. (a) Spatial distribution of the ~~seasonality~~ amplitude of the annual cycle of surface chlorophyll in log scale ($\log(\mathrm{chl}\ (\mathrm{mg\,m^{-3}})^{-1})$); (b) Map of annual mean upwelling velocity w ($\mathrm{m\,d^{-1}}$) at the bottom of the mixed layer, with contour lines indicating MLD (m). White lines highlight the focus area; (c) Taylor diagram for seasonal SST (red), MLD (yellow), surface nitrate concentrations (~~blue~~purple) and chlorophyll (green). The black dot indicates the model simulation as a reference. The radial distance from the origin is proportional to the standard deviation~~(normalized~~, normalised by the standard deviation of the data~~)~~. The green dashed lines ~~indicate~~ show the RMSE. The correlations between model and observations are given by the azimuthal position; (d) Seasonal cycles of surface chlorophyll concentration from model simulation (black solid line), satellite data (dotted line; SeaWIFS (diamond) and MODIS (square)) and ~~in situ~~ in-situ data (~~digitized~~ digitised from ~~Pennington et al. (2006, star)~~ Pennington et al. (2006, star, 250 km band off the coast) and Echevin et al. (2008, cross)).

Peruvian systems ($R^2 = 0.90$) feature replete surface nitrate over most of the year. ~~With~~ Because higher nitrate concentrations ~~correlated~~ correlate with lower chlorophyll ~~, this suggests that~~ in these cases, nitrate is not ~~limiting~~observed to be a limiting factor.

In the Peruvian system, a strong relationship exists between deepening mixed layers and decreasing chlorophyll (Fig. 2c, $R^2 = 0.91$), ~~supportive of~~ which supports the notion that dilution of phytoplankton over a deeper mixed layer and/or light limitation plays a role, as ~~suggested~~ found by Echevin et al. (2008). The California system shows a similar ~~albeit damped~~ response to mixed layer~~s~~ variations ($R^2 = 0.62$), suggesting that the same process may play a role ~~here, too. The weaker increase of phytoplankton concentrations with shallowing mixed layers compared to the Peruvian system is consistent with a greater role of nutrient limitation. The Benguela system, if at all (insignificant), shows a very weak response to mixed layer depth variations, despite quite some range of mixed layer depths over the course of the year. The Canary system does not feature~~

~~a substantial mixed layer depth variability. Rather, in the Canary system, mixed layers are shallow throughout the year, possibly contributing with favorable light conditions to comparatively high chlorophyll concentrations throughout the year. All in all,~~ ~~the Peruvian system shows the strongest response to MLD variations. Surface chlorophyll correlates positively~~ there as well. Additionally, surface chlorophyll shows significant correlation with SST in the Peruvian (Fig. 2d, $R^2 = 0.73$) and California systems ($R^2 = 0.65$)~~and to a lesser extent in the Benguela upwelling ($R^2 = 0.41$)~~, suggesting that increasing temperatures ~~are stimulating~~ stimulate phytoplankton growth. ~~The Benguela system also upholds the trend of increasing chlorophyll following the increasing temperature, though the correlation is not significant. As for MLD, the Canary system does not reveal a strong seasonal SST variance albeit features comparatively high SSTs throughout the year.~~

Strikingly, the Peruvian system is the only one of the four EBUS where high upwelling coincides with deep MLD (Fig. 2e, $R^2 = 0.79$). The Canary ~~system features a seasonality of upwelling but shallow mixed layers throughout the year, while the Benguela system does not vary much in terms of upwelling while varying in terms of~~ and Benguela systems exhibit pronounced seasonality either in upwelling or in mixed layer depth, respectively. In the California system, the relationship of upwelling and mixed layer depth is opposite to that of the Peruvian system, with the highest upwelling ~~into~~ occurring in the shallowest mixed layers.

Given the paradox that strong upwelling in the Peruvian system occurs at the time of the yearly chlorophyll minimum, it is intuitive that the concurrent deep mixed layers offset the positive impact of upwelled nutrients. ~~In other words, more nutrients only have a strong local positive effect if concentrations are low / would be low otherwise~~Nutrient enrichment would only stimulate higher productivity if the region was nutrient limited. If concentrations are already elevated, adding more nutrients ~~will~~ would have a weak impact. We will ~~look further into~~ further investigate the interplay of the seasonality of mixed layers and upwelling in the Peruvian system in the following sections.

3.2 Modelled phytoplankton biomass, dissolved inorganic nitrogen, upwelling and the MLD in the Peruvian system

We ~~use~~ used a regional ocean circulation model, coupled to a marine biogeochemical model (CROCO-BioEBUS), to further analyse the Peruvian system (see ~~Methods~~the "Data and Methods" section). The model ~~reproduces well~~ effectively reproduced the observed estimate of the seasonal out-of-phase relationship ~~of~~ between surface phytoplankton biomass ~~with upwelling intensity and~~ and upwelling intensity as well as nitrate concentrations (Fig. 2, open circles). ~~In the model~~Over the course of the year, surface chlorophyll~~and nitrogen concentrationstogether with~~ , surface nitrogen concentrations, upwelling intensity and MLD ~~all display a 40-60% seasonal variability~~varied by 40 - 60% relative to their annual mean values. Surface phytoplankton biomass concentration ~~is highest in~~ reached its maximum from late austral summer to early autumn (March to April)~~when upwelling is~~ , when upwelling was relatively weak (Fig. 3a,b). ~~Less~~ During this time window, less nitrogen is available within a shallow MLD compared with the rest of the year. In austral winter (July to September), when upwelling ~~brings up~~ introduces ample nitrogen into the deep mixed layer, surface phytoplankton concentration ~~is lowest~~reaches a minimum.

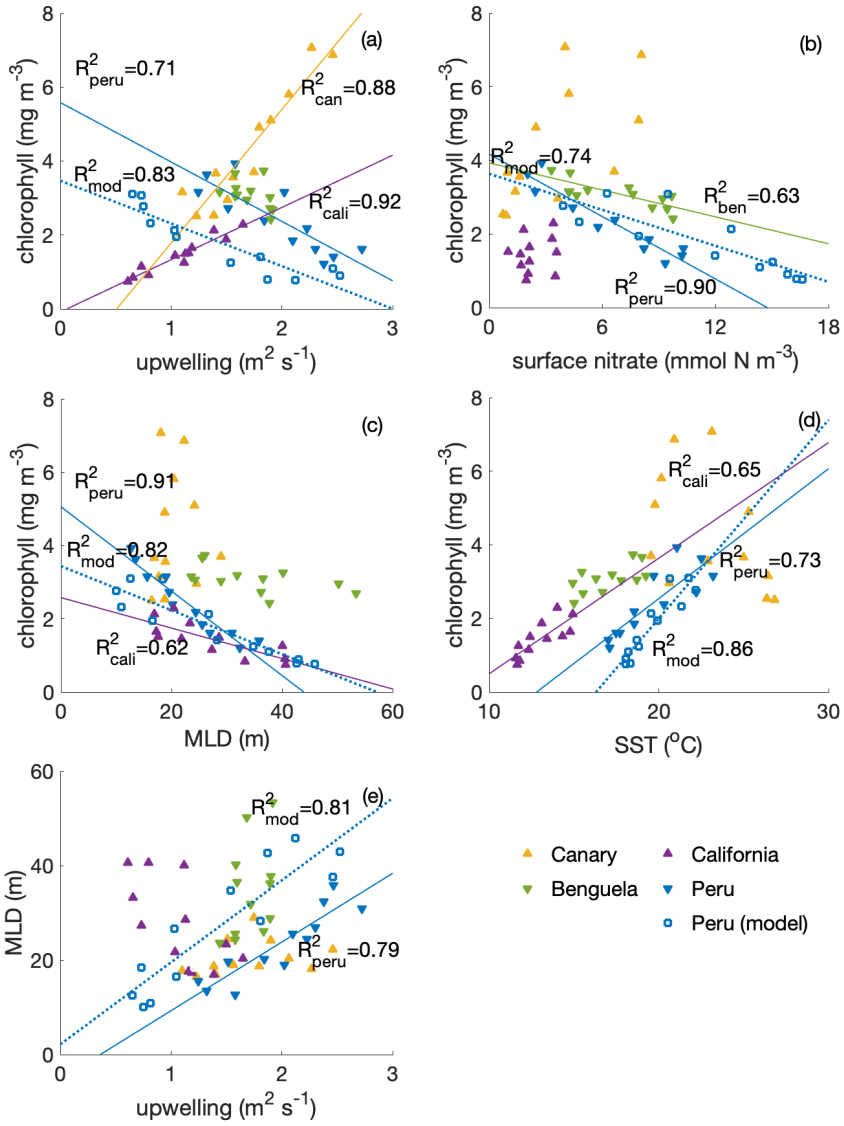

Figure 2. Correlations of surface chlorophyll (SeaWIFS climatology, in $\mathrm{mg\,m^{-3}}$) with (a) upwelling (a combination of Ekman transport and Ekman pumping, estimated based on winds from QuikSCAT, in Sv, ~~digitized~~ digitised from Chavez and Messié (2009), for calculations see Messié et al. (2009)); (b) surface nitrate concentration (WOA, in $\mathrm{mmol\,N\,m^{-3}}$); (c) MLD (ARGO, in m); (d) SST (MODIS, in $^\circ$C) and (e) correlation of MLD and upwelling transport among four eastern boundary upwelling systems (EBUS)~~; for~~. For the Peruvian system, we ~~show~~ also show the model (CROCO-BioEBUS) results. Lines and R^2 values are ~~given~~ displayed for correlations with $R^2 > 0.5$.

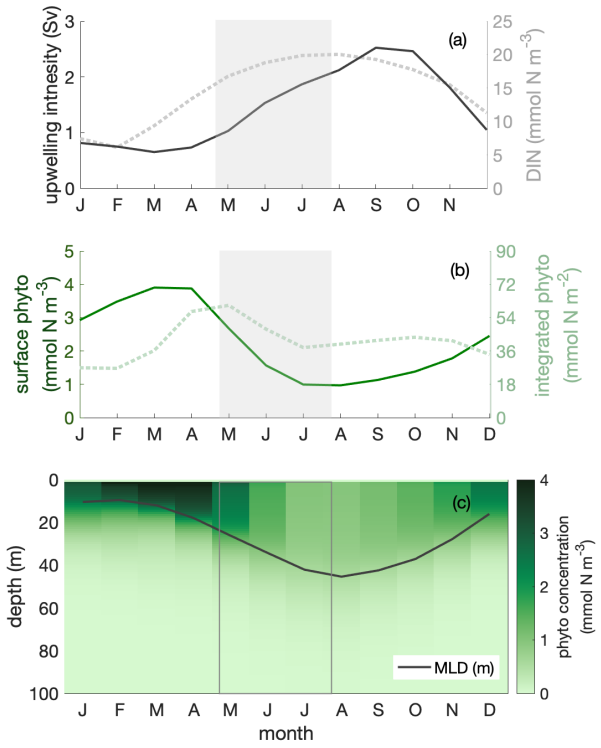

Figure 3. Seasonal cycles of (a) upwelling intensity (in Sv, solid line) and surface dissolved inorganic nitrogen (DIN) concentration (in $\mathrm{mmol\,N\,m^{-3}}$, dotted line); (b) surface (in $\mathrm{mmol\,N\,m^{-3}}$, solid line) and mixed layer depth (MLD)-integrated phytoplankton biomass (in $\mathrm{mmol\,N\,m^{-2}}$, dotted line); (c) phytoplankton depth-month distribution~~with~~, showing the seasonal cycle of MLD (in m, solid line) within the focus region. The shaded area indicates the decline phase of ~~MLD integrated~~ MLD-integrated phytoplankton biomass.

3.3 Biomass dilution by the deepening mixed layer

Dilution of phytoplankton in deepening winter mixed layers is a key driver behind the seasonality of surface phytoplankton concentration. Within the research area, the MLD ~~shows~~ showed a seasonal variation with the shallowest mixed layer in austral summer~~(~~, around 10 m~~)~~, and the deepest mixed layer in austral winter~~(~~, around 45 m~~). Phytoplankton is~~ . Phytoplankton were vertically well mixed within the mixed layer throughout the year (Fig. 3c). In austral winter, ~~in~~ within the 'deep-mixing' regime, phytoplankton ~~is~~ were evenly distributed over a relatively deep mixed layer, diluting phytoplankton biomass. Accordingly, phytoplankton biomass concentrations in the mixed layer ~~, and along with it~~ as well as at the surface ~~, decrease~~decreased. Hence, we infer that seasonal mixed layer deepening and shoaling alone is an important factor in driving phytoplankton concentrations at the ocean surface, as observed for instance ~~based on~~ from satellite images.

While dilution ~~causes a decrease of~~ caused a decrease in winter surface phytoplankton biomass, it ~~explains~~ explained only part of the observed biomass decrease~~: the decline persists~~. The decline persisted, even though attenuated, ~~if we integrate~~

when integrating phytoplankton over the mixed layer (Fig. 3b). The phytoplankton concentration at the surface ~~(~~and within the mixed layer ~~) declines~~ declined by around 70%~~while declines~~ , while it declined by around 30% for MLD-integrated biomass between late April and late July (shaded area in Fig. 3 & ~~4~~4, hereafter referred to as the decline phase). The decline of surface phytoplankton concentrations can be attributed to the decline due to the increase ~~of the~~ in mixed layer volume ΔV (dilution effect, see Eq. 5) and ~~a decrease of the~~ the decrease in biomass ΔB within the mixed layer ~~(~~through local biological and physical processes ~~,~~ (see Eq. 5). During the decline phase, ΔV ~~contributes~~ contributed by slightly more than half to the concentration change, while ΔB ~~contributes~~ contributed slightly less than half. That is, the dilution effect due to the deepening mixed layer in the decline phase ~~amplifies~~ amplified the decline of surface biomass concentrations by ~~about~~ approximately a factor of two. ~~Yet, dilution can~~ However, dilution could not fully explain the low phytoplankton biomass in conditions ~~of ample~~ where the supply of nitrogen is ample; in such conditions, MLD-integrated biomass still ~~declines by around 35~~declined by around 30%.

3.4 Biological and physical processes change the total biomass within the mixed layer

3.4.1 Disentangling physical and biological processes

~~Besides~~ In addition to causing dilution due to the deepening mixed layer, the imbalance of a series of biological and physical processes during the decline phase ~~also diminishes~~ diminished phytoplankton concentrations. To disentangle their contributions to the decline of phytoplankton concentration without the ~~complication~~ complicating factor of the dilution effect, we next ~~analyze~~ analysed the change of phytoplankton biomass integrated over the mixed layer (Fig. ~~4~~4a) and its drivers~~, that is~~; that is, the mixed layer budget of phytoplankton biomass (Eq. 1~~, Supplementary Fig. C2~~). We ~~separate~~ separated biological processes (e.g., primary production, grazing from zooplankton, natural mortality, exudation ~~,~~ and sinking) and physical processes (mixing, advection and entrainment) that affect the integrated biomass~~(Fig. 4b).~~ . Throughout the year, the net biological flux ~~is positive , acting as a source for MLD-integrate phytoplankton biomass, while~~ (the sum of all biological fluxes) was positive ("biological gain", Fig. 4b), thus supporting an increase in biomass. In contrast, the net physical flux~~is negative , acting as a sink. The balance of these terms determines if the total biomasswithin the mixed layer decreases or increases. Most biological and physical processes decrease from the start (t1) to the end~~ , the sum of all physical fluxes, was negative ("physical loss"), therefore supporting a decrease in biomass. The time point t1 marks the seasonal maximum of the MLD-integrated phytoplankton biomass, and t2 ~~)~~ marks the minimum at the end of the decline phase. At t1 and t2, the net biological and physical fluxes balanced (Fig. ~~4c-d). While mortality is larger at t2 than t1,it is only due to a sudden increase by the end of the decline phase~~ 4b,c) and the tendency of the mixed layer phytoplankton biomass was zero (Fig. ~~C2). The more rapid decrease of net biological source relative to net physical loss leads to biomass reduction during the decline phase~~ 4a). Between t1 and t2 (Fig. ~~4b)~~4b), the net biomass supply due to biological fluxes decreased more quickly than the net biomass removal due to physical fluxes, resulting in an imbalance of the fluxes and the decrease in biomass between t1 and t2.

~~The biological and physical processes that promote a decline of the MLD-integrated biomass are a reduction of primary production and entrained phytoplankton, along with an enhanced phytoplankton offshore transport~~ To determine which terms

from Eq. 1 mostly drove the decrease of the biomass between t1 and t2 (Fig. ~~4e-f). Among the biological processes, the reduction of primary production as the only source process overpowers the weakening of biological sink processes and significantly promotes the biomass decline. Within the physical processes, the net effect of lateral and vertical transport of phytoplankton biomass (advection)is picking up~~ 5a), we integrated the change of each term over time (that is, the derivatives) between t1 and t2. Therefore, in Fig. 5b and c, if a bar was positive (red), the change of the term during the decline phase ~~, leading to a net offshore export of phytoplankton biomass. In addition, while phytoplankton is entrained into the mixed layer from below when mixed layers deepen, the rate of entrainment decreases~~ (t1 - t2) promoted an increase of the phytoplankton biomass, mostly as a result of reduced grazing pressure and reduced downward mixing. If the bar was negative (grey), the change of the term during the decline phase (t1 - t2) opposed an increase in phytoplankton biomass. The "opposing terms" that acted to reduce phytoplankton biomass were the ones that contributed to the seasonal paradox; that is, decline in biomass despite increased supply of nutrients due to upwelling. These terms mostly referred to the reduced primary production, with a secondary contribution from the reduced convergence due to advection, as well as a small effect due to detrainment. ~~The decreasing rate is due to decreasing phytoplankton concentrations at the bottom of mixed layers as mixed layers deepen. All other biological and physical processes act to oppose the decline of phytoplankton biomass , such as an attenuation of mixing out of the mixed layer over the decline phase.~~ Details regarding the two major contributors, primary production and advection, are presented in the following sections.

3.4.2 Factors limiting primary production

Primary production ~~changes~~ changed due to variations ~~of~~ in both the growth factor and the biomass (Eq. 2). The growth factor (calculated as in Eq. 3, Fig. 6a) ~~combines~~ combined the effects of light, temperature and nitrogen on phytoplankton growth. It ~~shows~~ showed a clear decrease ~~(~~of around 30% ~~)~~ during the decline phase. Optimal phytoplankton growth conditions ~~are~~ were reached in March, despite the low dissolved inorganic nitrogen (DIN) conditions, ~~with~~ within the warmest and brightest environment. The lowest growth rate ~~occurs~~ occurred just after the decline phase, despite relatively high nitrogen concentrations, due to limiting light and temperature conditions.

Strong light limitation experienced by phytoplankton, in combination with low temperatures~~slows down the~~ , slowed growth during the decline phase. Light conditions for phytoplankton growth ~~are best~~ were optimal in March when the water ~~is~~ was rather stratified and ~~worsens~~ worsened over the decline phase to a minimum in August when the water column ~~is mixeddeepest~~was most deeply mixed. The light-related growth factor ~~declines~~ declined by 17% during the decline phase and would decrease the growth factor by ~~around~~ approximately 60% in the absence of other limiting factors~~(estimated based on~~ , estimated from Eq. 3~~). The decreasing temperature is~~ . Decreasing temperature was the second most important ~~factor to slow~~ contributor in slowing the growth rate ~~in~~ during the decline phase. The temperature-related growth factor ~~reaches~~ reached its maximum by March, ~~similarly~~ similar to the light-related growth factor, and reached its minimum by October. The temperature-related growth factor ~~declines~~ declined by 12% and would decrease the growth factor by around 40% during the decline phase, in the absence of other limiting factors~~during the decline phase~~. In contrast, the seasonality of the growth factor

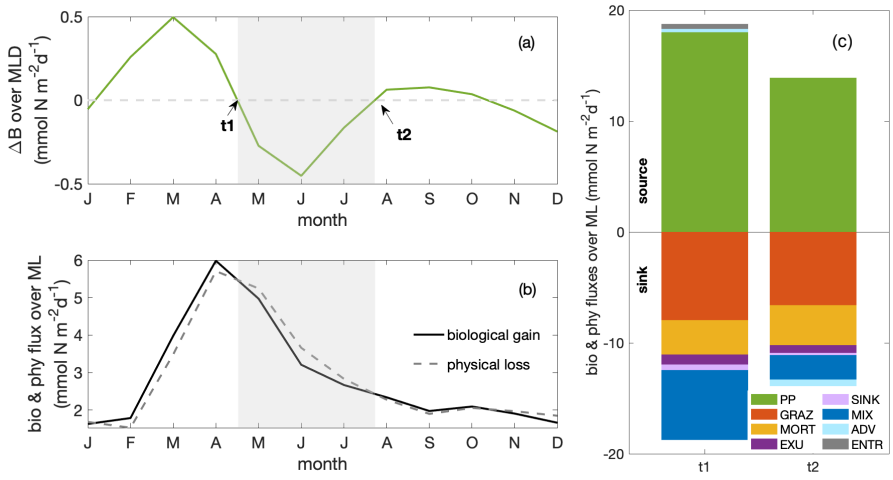

Figure 4. Seasonal cycles of (a) total phytoplankton biomass change (ΔB; in ~~the mixed layer (in~~ mmol N m^{-2} d^{-1}~~);~~ ~~gray~~. Grey shading indicates the decline phase~~as in Fig. 3~~, with ~~t_1~~ t1 and ~~t_2~~ t2 marking the beginning and end of the decline phase; (b) ~~MLD-integrated~~ phytoplankton fluxes resulting from net biological gain (bio) and net physical ~~fluxes~~ loss (phy, in mmol N m^{-2} d^{-1}, as shown in Eq. ~~1~~ 1 plus the entrainment and detrainment introduced by the ~~integration~~temporal variation of the MLD); ~~bar plots of~~ (c) ~~biological and (d) physical fluxes~~ Stacked bar plots displaying balancing budgets at ~~the start (~~t1 ~~, light green)~~ and ~~end (~~t2~~, dark green) of decline phase; bar plots of the integrated change over the decline phase over mixed layer due to (e) biology and (f) physics within the focus region~~. ~~Red and grey indicate promoting and opposing ML-integrated phytoplankton biomass decline. pp~~ PP stands for primary production; ~~graz~~ GRAZ for consumptive mortality; ~~mort~~ MORT for natural mortality; ~~exu~~ EXU for exudation; ~~sink~~ SINK for sinking; ~~mix~~ MIX for mixing; ~~adv~~ ADV for advection and ~~entr~~ ENTR for entrainment. Fluxes are distinguished as sources (positive values) and sinks (negative values) of phytoplankton biomass, with the sum of all source and sink terms balancing at times t1 and t2. All fluxes are integrated over the MLD.

due to nitrogen ~~shows~~ showed the opposite seasonality compared to the total growth factor. Clearly, light and temperature ~~regulate~~ regulated primary production and ~~override~~ overrode the effect of nitrogen supply during the decline phase. Therefore, while light ~~is~~ was the dominant mechanism that ~~reduces~~ reduced productivity towards winter, we ~~find that temperature plays~~ found that temperature played a relevant secondary role.

Stronger light and temperature limitation during the decline phase ~~are~~ were due to deeper mixing and stronger upwelling of cold waters, respectively (Fig. 6b-c). While upwelling intensity ~~is~~ was approximately correlated with ~~deep mixed layers occurring when upwelling is high, the peak of upwelling happens~~ MLD, the maximum upwelling occurred just after the deepest mixed layers. The variation of MLD-averaged light limitation ~~is~~ was correlated ($R^2 = 0.92$) with the change of MLD. As phytoplankton ~~is~~ were evenly distributed within the mixed layer, deeper MLD ~~means more phytoplankton is exposed to a relatively lower light condition on average in~~ indicated that, on average, more phytoplankton were exposed to lower light conditions during the decline phase, with a minimum in August when mixed layers ~~are~~ were deepest. The change of the temperature-related growth factor within the mixed layer ~~is closely related ($R^2 = 0.83$)~~ was closely related with the seasonal

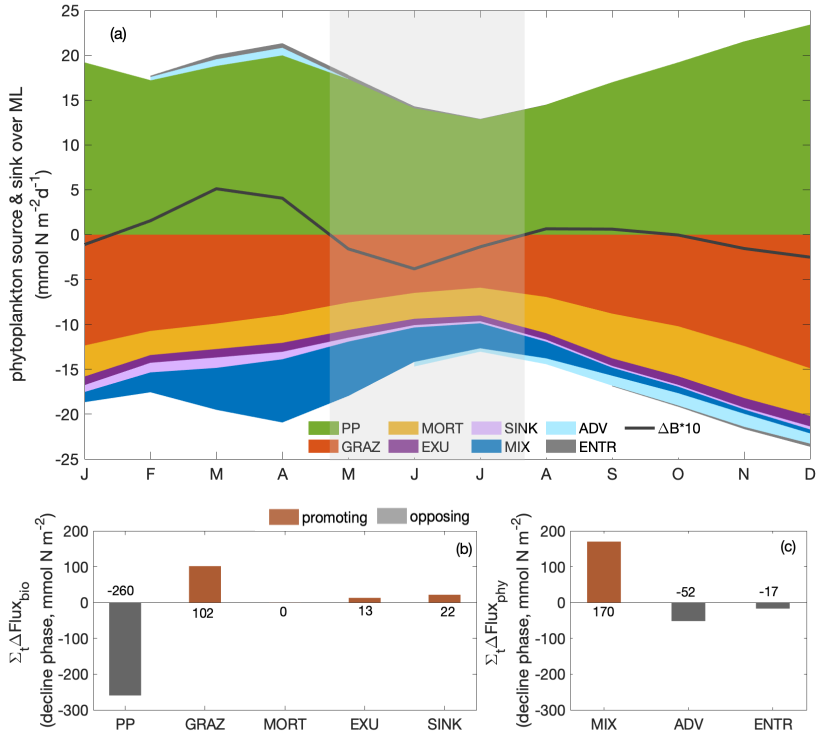

Figure 5. (a) Seasonal cycle of phytoplankton source and sink processes, as well as phytoplankton biomass change (ΔB multiplied by a factor of 10; solid line); bar plots of the integrated change over the decline phase due to (b) biological fluxes and (c) physical fluxes averaged over the focus region. Red and grey shading indicate fluxes promoting and opposing an increase in MLD-integrated phytoplankton biomass, respectively. The magnitude of the integrated change is given as numbers above and below the bars. PP stands for primary production; GRAZ for consumptive mortality; MORT for natural mortality; EXU for exudation; SINK for sinking; MIX for mixing; ADV for advection and ENTR for entrainment. All fluxes are integrated over the MLD.

variation of upwelling intensity ($R^2 = 0.83$), with the lowest values occurring in September and October when upwelling intensity ~~is highest. In~~ reached its maximum. During the decline phase, cold waters ~~are~~ were upwelled into the mixed layer at a higher rate, further damping phytoplankton growth in addition to the effects of limiting light conditions. Reduced winter surface solar radiation and heat loss to the atmosphere ~~, also play~~ also played a role in the seasonality of the light and temperature growth factors, respectively (Fig. C2), ~~yet of much less importance~~ though to a much smaller extent (not shown).

3.4.3 Enhanced upwelling and offshore transport of phytoplankton

An enhanced advective loss of mixed layer phytoplankton is a second-order process, promoting the decrease of MLD-integrated phytoplankton biomass during the decline phase. ~~Like~~ Similar to the effects of nutrients, phytoplankton biomass is affected by the seasonality of upwelling and offshore export of waters. ~~Phytoplankton growing at the bottom~~ Relatively dilute concentrations

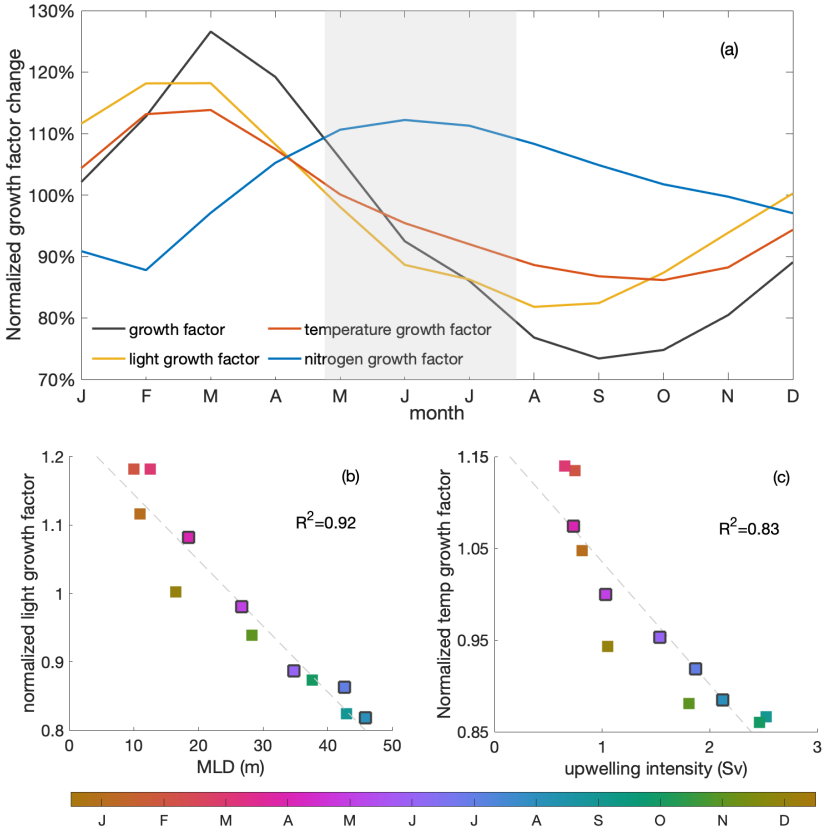

Figure 6. (a) Seasonal cycles of the ~~normalized~~ normalised total (black) growth factor ~~,~~ and light (yellow)-, temperature (red)- and nitrogen (blue)-related growth factors ~~, as experienced by~~ for phytoplankton over the mixed layer. The grey shading indicates the decline phase~~;~~. (b) ~~seasonal~~ Seasonal correlation of MLD and mixed ~~layer averaged~~ layer-averaged light-related growth factor; (c) correlation of upwelling intensity and mixed ~~layer averaged~~ layer-averaged temperature-related growth factor. ~~Colors~~ Colours indicate the time of the year (months), with black edges ~~marking~~ indicating the months of the decline phase. The R^2 ~~value~~ values of the ~~correlation is~~ correlations are shown in the ~~right of~~ right-hand sides within the panels.

of phytoplankton growing below the base of the mixed layer ~~is being upwelled and later pushed offshore along with the phytoplankton that is growing in the mixed layer~~are upwelled into the mixed layer, while waters with mixed-layer-averaged phytoplankton concentrations are pushed offshore. During the decline phase, the upwelling and offshore transport of water ~~increases and more of what is~~ increased and a greater volume of what was produced in coastal waters ~~is~~ was exported offshore: 4% of primary production ~~is~~ was lost via advection by the end of the decline phase compared to 2% gained at the beginning. This greater loss of biomass due to divergent ~~advection is~~ lateral advection was mainly caused by stronger upwelling ~~in~~ during the decline phase (Fig. C3).

3.5 Seasonal Paradox: from phytoplankton to export

Small and large zooplankton exhibit the same "seasonal paradox" pattern as phytoplankton, and so does the export of organic material to the deeper ocean. Similar to phytoplankton, both small and large zooplankton are vertically well mixed within the mixed layer throughout the year (contours and colours in Fig. 7a, respectively); biomass concentrations are high in austral summer and low in austral winter, in opposition to the upwelling trend. Additionally, the particulate organic matter, the sum of plankton biomass and other organic particles, follows the same pattern, with large amounts of particulate organic matter concentrated in a shallow mixed layer during the productive summer (Fig. 7b). The pattern of organic matter in the water column is then reflected in the export pattern of sinking organic material, composed of large phytoplankton as well as small and large detritus (Fig. 7c). Export below 100 m depth is high during the productive summer, when the mixed layer is shallow and particulate organic matter is large, and low in winter (Fig. 7b, black line). That is, the model's ecosystem is affected by the seasonal variation of the MLD.

Finally, export efficiency also follows the seasonal cycle of the MLD. Export efficiency is defined as the export of sinking organic material through the 100 m depth level, relative to primary production in the upper 100 m. It reaches a maximum in austral summer, when MLD is shallow, and a minimum in austral winter, when MLD is deep (Fig. 7d). As both export and primary production show the same seasonal trend as phytoplankton biomass, export must overcompensate the change in primary production and vary even more, in order to allow export efficiency to reveal the same seasonal trend. Export largely consists of large detritus originating from large zooplankton faecal pellets and mortality (Fig. 7c). Since large detritus possesses the fastest sinking speed compared to other components, it sinks the most efficiently. The relative contribution of fast-sinking large detritus to total export is largest in summer, close to 100 %, which may partially explain the higher export efficiency. In addition to changes in composition of the sinking organic material, other processes may cause export to be amplified relative to phytoplankton production. These include: (1) changes in structure and trophic transfer efficiency of the plankton food web, and (2) a varying degradation of sinking organic matter in the upper 100 m, that is, differences in the remineralisation. The detailed mechanisms behind the seasonality of export efficiency are beyond the focus of this paper and will be investigated in a separate study.

4 Discussion

4.1 Mixed layer depth drives surface phytoplankton biomass seasonality in the Peruvian upwelling system

The regional ocean circulation-biogeochemical model that we ~~use successfully reproduces~~ used successfully reproduced the "seasonal paradox", ~~with~~ defined as the seasonal out-of-phase surface chlorophyll concentration and upwelling intensity, as derived from observations. As shown in the results, the low surface chlorophyll concentration in high upwelling conditions ~~in austral winter is~~ during austral winter was constrained by a combined effect of MLD-driven ~~processes~~ and upwelling-driven processes. Under ~~high upwelling conditions in~~ strong upwelling conditions during austral winter, phytoplankton ~~is~~ were diluted over a deeper mixed layer, leading to a decrease ~~of~~ within the mixed layer~~, and likewise,~~. Likewise, surface phytoplankton

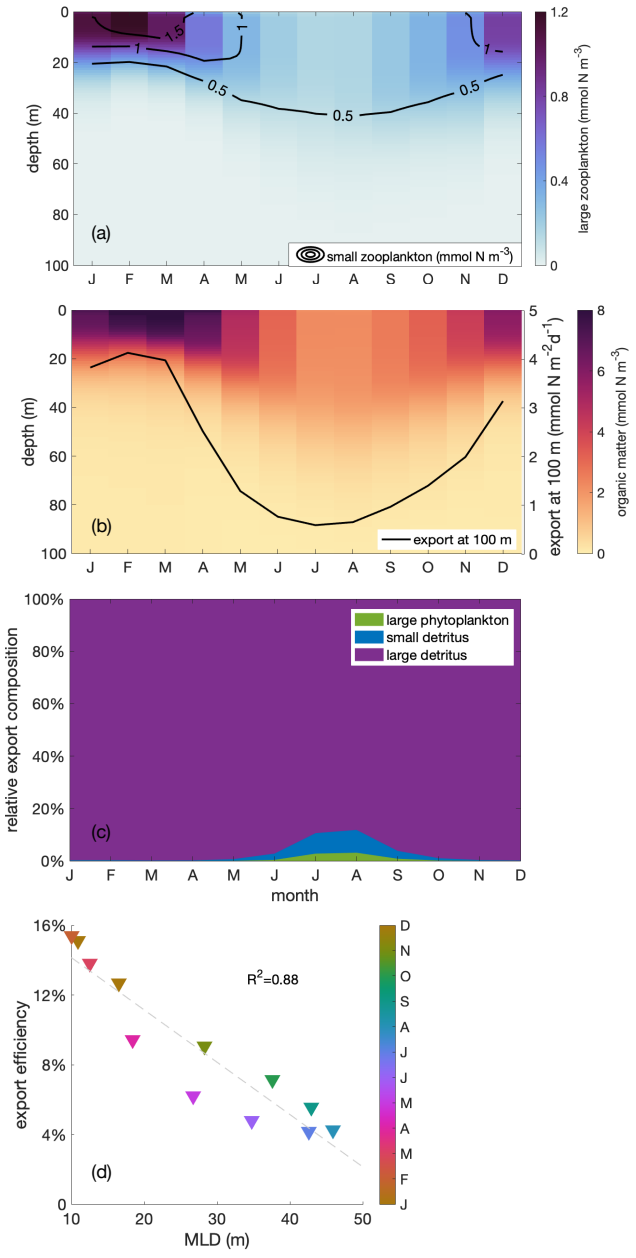

Figure 7. Monthly depth distribution of (a) large and small zooplankton (in colours and contour lines, respectively) and (b) organic matter with the seasonal cycle of vertical export through the 100 m depth horizon (black line); (c) Seasonal cycle of the relative contributions to sinking organic matter from large phytoplankton (green) and small (blue) and large (purple) detritus; (d) correlation of export efficiency with mixed layer depth (MLD) within the focus region. The export efficiency is defined as the ratio of export through the 100 m depth level to primary production in the upper 100 m. Colours indicate the month of the year.

concentrations decreased by over 50%. Also, phytoplankton growth ~~is slowed down as they experience~~ was slowed due to deteriorating light and temperature conditions~~. On top of that, strong upwelling pushes~~ , as well as strong upwelling pushing phytoplankton offshore.

Several previous studies have also focused on the possible reasons behind the seasonal paradox in the PUS. Echevin et al. (2008) also ~~suggested based on model results that relative~~ used a regional ocean circulation-biogeochemical model to examine the reasons for the relatively low surface chlorophyll concentration ~~in austral winter~~ off the Peruvian coast ~~is~~ in austral winter. Based on a series of model sensitivity experiments regarding vertical mixing, surface temperature, iron limitation and insolation cycle, Echevin et al. (2008) concluded that the low surface chlorophyll in austral winter is mainly generated by the combined effect of dilution and deteriorating light ~~limitation~~ with deepening mixed layers. ~~In addition, Messié and Chavez (2015) find~~ Additionally, the iron sensitivity experiment confirmed the existence of iron limitation in austral winter, which corroborated the findings in Messié and Chavez (2015). Messié and Chavez (2015) pointed out that more severe iron limitation under low light ~~condition~~ could also be one of the reasons behind low primary production under ~~high~~ strong upwelling conditions. According to results from culture experiments, phytoplankton iron demand would increase under light limitation ~~conditions~~ (Sunda and Huntsman, 1997). Based on observations, Friederich et al. (2008) ~~suggest~~ suggested that winds in the ~~winter~~ high-upwelling ~~conditions favor curl driven~~ winter conditions favour curl-driven offshore upwelling, which would draw more offshore iron-deficient waters to the surface. On the contrary, a model study (Albert et al., 2010) ~~finds that stronger wind-curl driven upwelling actually is recruiting~~ found that stronger wind-curl-driven upwelling actually recruits more nutrient-rich water from a shoaling coastal undercurrent, thus ~~contributing to~~ enhancing surface chlorophyll concentrations. We ~~cannot~~ could not assess the role of iron in regulating the seasonality of phytoplankton biomass because our biogeochemical model ~~does~~ did not simulate iron~~(see Sect. B).~~. Nevertheless, our study ~~confirms~~ confirmed the importance of vertical redistribution of biomass and light limitation due to vertical mixing. ~~Here, we emphasize the importance of the deepening mixed layers in the decline phase.~~

4.2 Upwelling into deep mixed layers: A unique feature of the Peruvian upwelling system and its implications

As ~~we just argued~~ stated in the previous paragraphs~~using the differences of~~ , based on the differences in the seasonalities of MLD and upwelling in the Peruvian system~~. The upwelling of nutrient rich waters happens~~ , upwelling of nutrient-rich waters occurs when growth conditions are ~~the worst, i.e.~~ least optimal, in particular when light availability is lowest due to deep mixed layers. ~~Also, the upwelled waters are comparatively cool and in deep mixed layers may warm up relatively slowly. At the same time, the upwelling will charge the deep mixed layers with nutrients that allow for growth once the mixed layer shallows. That is, the upwelling into deep mixed layers in the Peruvian may precondition high summer phytoplankton production.~~

In contrast, ~~in~~ within the California system, nutrients are upwelled into the shallowest mixed layers. While this nutrient supply coincides with shoaling mixed layers~~and associated~~ , associated with improved light conditions and reduced dilution, it does not result in as high a level of phytoplankton concentrations as for the Peruvian system. This supports that nutrient limitation ~~is important~~contributes substantially to processes in the California system, as the supply of nutrients to shallow mixed layers ~~by upwelling appears~~ through upwelling appears to be insufficient to relieve nutrient limitation. ~~We speculate that the charging of deep mixed layers as in the Peruvian system is more efficient in supplying nutrients to the euphotic zone~~

compared to upwelling into shallow waters as in the Californian system, possibly warranting further studies. Also, Additionally, if nutrients are being upwelled into deep mixed layers and allow the onset of a bloom, zooplankton standing stock stocks might be low and take a while require more time to catch up and eventually reduce , eventually reducing phytoplankton biomass. On the contrary, if nutrients are being upwelled into shallow mixed layers, zooplankton standing stock is probably already high and zooplankton can act on the spot to limit stocks are likely already elevated, allowing zooplankton to immediately limit any increase in phytoplankton biomass.

While the Canary and Benguela systems lack a pronounced seasonality in MLD and phytoplankton, respectively, we mark point out a few aspects that may point towards a elucidate the role of MLD also in these systems. Given that the Canary system does not feature a substantial seasonal MLD variability, it is intuitive that it phytoplankton follows the seasonality of upwelling intensity more strongly compared to the other EBUS. While mixed layer conditions do not modulate the seasonality of phytoplankton, they may contribute to Canary high phytoplankton concentrations in the Canary system insofar as mixed layers are shallow throughout the year, creating favorable favourable light conditions. Finally, the Benguela system features a rather constant upwelling through throughout the year into varying mixed layers. The non-responsiveness unresponsiveness of phytoplankton to the varying MLD hypothetically could could hypothetically be due to compensating effects of deepening mixed layers that dilute phytoplankton and deteriorate light conditions, but the same time are accompanied by are simultaneously accompanied by an enhanced supply of nutrients that are is mixed up from below. The higher surface nitrate concentrations in conditions of deep mixed layers in the Benguela system could be interpreted this way. Enhanced growth due to higher nutrient availability would then offset, yet not completely, the worsening light conditions and dilution. Finally, the strong response of phytoplankton in the Peruvian upwelling system to mixed layer depth would then be due to the unique situation of upwelling into deep mixed layers.

Again, other Other factors may also play a role in contribute to regulating phytoplankton in the EBUS next to aside from nutrients, dilution and light associated with upwelling and MLD (see also Results section; Messié and Chavez, 2015) (also see the Results section; Messié and Chavez, 2015), including the advection of biomass and regulation by temperature that varies with upwelling (see Results). In addition, Lachkar and Gruber (2011) suggest that a longer residence time because of a wide shelf and weak mesoscale activity may also promote phytoplankton growing. Also, next growth in the Canary system. Next to iron supply from the shelves and upwelling of source waters, Fung et al. (2000) also found that atmospheric deposition of iron varies between EBUS.

4.3 From phytoplankton to Seasonal paradox and ecosystem functioning

The interplay of mixed layer depth and upwelling that leads to the seasonal paradox in the PUS is further propagating propagates further up the food chain and modulates , modulating the trophodynamics. In austral summer, when the shallow mixed layer along with the add-on effect from upwelling supports the highest phytoplankton biomass and primary production, it provides providing an ideal feeding place for zooplankton. In contrast, in winter zooplankton is facing during the winter zooplankton face a food shortage, less efficient grazing due to dilution and transports , and transport offshore due to enhanced upwelling. Similar to the spatial match-mismatch observed for phytoplankton and top predator in predators in the Benguela

system (Grémillet et al., 2008), mesozooplankton with ~~its slower growth rate~~ their slower growth rates may also be ~~affected by upwelling, with phytoplankton thriving near the coast and zooplankton concentrated further offshore.~~ negatively affected by enhanced upwelling.

In our model, mesozooplankton ~~is~~ are responsible for the major part of the export in the coastal upwelling region. During the productive season, the faecal material of mesozooplankton accounts for close to 100% of the sinking matter, which is in good agreement with what ~~is found in Stukel et al. (2013)~~ Stukel et al. (2013) observed for the California system.

Both primary production and export ~~are found to be determined by~~ can be determined from the mixed layer dynamics and ~~foodweb structures~~food web structures(Ducklow et al., 2001; Turner, 2015; Steinberg and Landry, 2017). The efficiency of the export, defined as the ratio of export to primary production, is also related to trophodynamics. ~~Export efficiency depends, as~~ We find that export efficiency is positively correlated with MLD on a seasonal scale. As mentioned above, it partially depends on the composition of the exported material. ~~In the PUS, it is positively correlated with net primary production (Fig. C5). Mesozooplankton produces~~ Mesozooplankton produce fast-sinking large detritus, which enhances the export efficiency during the productive season. ~~In both the Peruvian and California systems, high primary productivity coincides with a shallow MLD. What is different in the California system compared to the Peruvian system is that in the former the time of shallow mixed layers and high primary productivity is also the time of strongest upwelling. Strong upwelling and offshore transport may lead to the above mentioned spatial mismatch between phytoplankton and mesozooplankton, because mesozooplankton grows more slowly. This may then result in comparatively low large detritus despite high primary production. Therefore, high primary production may not necessarily tie in with high mesozooplankton biomass and subsequent high export. Indeed,~~ Kelly et al. (2018) observed that export efficiency is negatively correlated with net primary productivity in the California system. ~~However, they suggested that this negative correlation~~ They suggested that the negative correlation in the California system arises from a seasonal decoupling of export and particle production through long-lived ~~, slowly sinking particles that would~~ particles that introduce a temporal lag of mesozooplankton production and export to depth. ~~In addition, Henson et al. (2019) find~~ Henson et al. (2019) also identify a negative correlation between export efficiency and primary productivity on a global scale. They imply in their study that ~~it is~~ not just the phytoplankton community, but also the ~~foodweb structure~~food web structure, is important to export efficiency. Currently, it is not entirely clear why the PUS export efficiency behaves differently. We suggest that the ~~role of the~~ interplay of the mixed layer and upwelling in EBUS and ecosystem functioning ~~is closely linkedand warrants~~ are closely linked, warranting further examination.

4.4 ~~Potential change under global warming~~

~~Our findings suggest that for an assessment of the response of the EBUS to climate change, it is important to consider the potential change of the interplay between the mixed layers and upwelling dynamics. Phytoplankton will inevitably be influenced by climate change, responding to the changes in the biotic and abiotic environment. Impacts in a changing climate will arise from changes of stratification and upwelling that further lead to shifting growth conditions due to changes of light, temperature and nutrient (Behrenfeld, 2014). Previous observations indicate that waters near the coast have cooled since the 1950s, possibly due to an increase in upwelling (Gutiérrez et al., 2011). A recent regional modelling study (Echevin et al., 2020)~~

projects an intensive surface warming along with a weakening of wind-driven upwelling. While studies typically focus on changes in upwelling, our results suggest that MLD changes maybe even more relevant. Assuming that winds will never cease entirely and hence there will always be some upwelling that recharges the mixed layer with nutrients, shoaling of the mixed layer caused by intensive surface warming may dominate the response of phytoplankton and ecosystem functioning. A shoaling MLD may release the phytoplankton from the strong dilution and light limitation in austral winter, along with better light and temperature condition in austral summer, leading to the expectation of an attenuation of the seasonal paradox in future. While modulation of growth conditions due to changing temperatures and nutrient supply from changing upwelling also may play a role, Echevin et al. (2020) simulations suggest that surface chlorophyll overall will increase in the PUS due to global warming.

5 Conclusions and potential implications

In summary, CROCO-BioEBUS performs well compared with respect to observational data and successfully reproduces the "seasonal paradox" with an out-of-phase relationship of between surface chlorophyll and upwelling intensity in the Peruvian coastal waters. The In agreement with an earlier model study (Echevin et al., 2008), the seasonal cycle of surface chlorophyll concentration in our simulations is driven mostly by MLD-related processes(, specifically dilution and light limitation), with . Furthermore, our model results provide evidence for secondary contributions from upwelling-related processes (such as temperature limitation and advection). Unlike other EBUS, the PUS features a unique positive correlation of the mixed layer and upwelling, with the strongest upwelling into the deepest mixed layers, whose combined impacts lead to the seasonal fluctuation of surface chlorophyll concentration. . This is consistent with Lachkar and Gruber (2011) and Messié and Chavez (2015), who suggested that advection is relevant to the seasonal cycle, but in contrast to Echevin et al. (2008), who found that temperature was not important. Differences in results from Echevin et al. and our results likely originate in the different biogeochemical model components (e.g., different parameterisations of temperature dependencies of phytoplankton growth). Given the disparity of the models, the role of temperature limitation in the PUS warrants further investigations in order to better constrain second-order drivers of the seasonal paradox. The sensitivity of the different processes within the plankton ecosystem to temperature, as well as their interplay, are topics of active research (e.g. Thomas et al., 2017; Chen and Laws, 2017; Morán et al., 2018; Marañón et al., 2018;Barton and Yvon-Durocher, 2019) and relevant particularly in light of global warming.

We find that the seasonal variability of phytoplankton further propagates up the food chain and affects the trophodynamics , and ultimately export efficiency. Therefore, is reflected in trophodynamics and ecosystem functioning. In particular, zooplankton and organic matter within the water column mirror the seasonal cycle of phytoplankton. Finally, export and export efficiency are well-correlated with the MLD over the course of the annual cycle. Given that changes in MLD are correlated to many ecosystem components related to plankton ecosystem functioning, we argue for a more thorough understanding of the interactions behind the mixed layer and upwelling dynamicsalong with the , along with food web processeswill . A better understanding of how the interplay of MLD and upwelling impacts the ecosystem in the contemporary PUS will ultimately help to better project how coastal upwelling ecosystems, and in particular the Peruvian system, may vary under climate change.

Phytoplankton will inevitably be influenced by climate change, responding to changes in the biotic and abiotic environment. Impacts in a changing climate will arise from changes in stratification and upwelling, that further lead to shifting growth conditions due to changes of light, temperature and nutrients (Behrenfeld, 2014). A recent regional modelling study (Echevin et al., 2020) projects a weak decrease in upwelling along with increasing stratification in the PUS due to climate change. Our results suggest that the decreasing upwelling and increasing stratification will both contribute to an increase in surface phytoplankton, in agreement with the findings of Echevin et al. (2020). While a reduction of upwelling might lead to a reduced supply of nutrients, the region is far from being nutrient limited. Therefore, a reduction in upwelling could rather have an effect via temperature, reducing the cooling effect of upwelled waters. We hypothesise that the coastal region would experience more phytoplankton growth and biomass buildup with a reduction of upwelling, due to warmer surface waters and weaker offshore advection compared to the current environmental situation. According to our results, shoaling of the mixed layer will be more relevant than a decrease in upwelling intensity, reducing the dilution of phytoplankton and the light limitation in austral winter. This could possibly lead to an attenuation of the seasonal paradox in the future. As export and export efficiency are also regulated by MLD dynamics, we expect not only enhanced export but also an increase in the fraction of primary production that is transported to the deep ocean under global warming.

Code availability. CROCO and BioEBUS models are available at http://www.croco-ocean.org

Data availability. The model data used in this paper are available via the corresponding author

Appendix A: Methods

A1 Two-way nesting approach

Figure A1 ~~visualizes~~ visualises the coarser-resolution parent and nested finer-resolution child domain that contains the focus region. The variables in section B are shown for the child domain.

A2 Adjustment of biogeochemical model parameters

The parameter setting is the same as in José et al. (2017), with only a few biological parameters adjusted to make the ecology (phyto- and zooplankton biomasses, productivity) better fit observational data. The changed parameters along with value ranges from literature are listed in Table A1 and will be further explained below.

Here, we assign a higher mortality rate for large phytoplankton to simulate the potential impact of virus infection during bloom conditions (Suttle, 2005). Simulated phytoplankton biomass and its seasonality has been calibrated and evaluated against chlorophyll concentration data from MODIS monthly climatology data (https://oceancolor.gsfc.nasa.gov/). Nitrate has been evaluated based on WOA and cruise data while simulated MLD has been validated against the ARGO mixed layer database

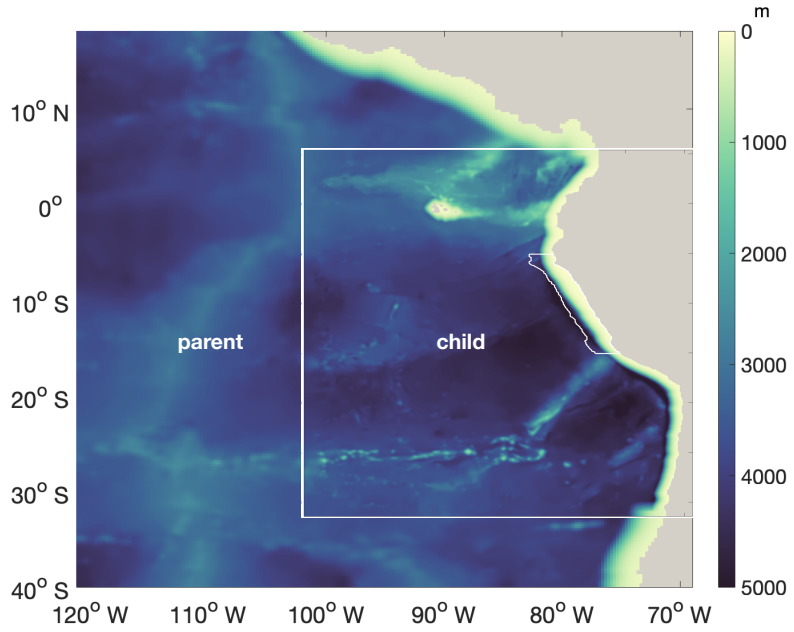

Figure A1. Bathymetry of the "parent" (1/4° resolution) and "child" (1/12° resolution) domains. White lines near the coast highlight the focus region.

(Holte et al. (2017), http://mixedlayer.ucsd.edu/).

Appendix B: Model evaluation

B1 Surface chlorophyll concentration

The large-scale spatial pattern of annual average surface chlorophyll of the monthly climatology of MODIS data and CROCO-BioEBUS are similar (Fig. B1), with higher chlorophyll concentrations in coastal regions and lower concentrations offshore (note that chlorophyll is shown in log-scale). The satellite data features a higher cross-shore chlorophyll concentration gradient compared to the model simulation. The model's overestimation of the low offshore chlorophyll and hence weaker cross-shore gradient potentially is due to the lack of iron limitation in the model. Apart from that, the model is also not able to correctly capture the alongshore pattern (Fig. B1), i.e. it misses two observed high surface chlorophyll concentration patches between 8°S to 10°S and 12°S to 14°S (Bruland et al., 2005). Within a 200 km band near the coast, both satellite data and the model simulation show a similar seasonality with maximum chlorophyll concentrations exceeding 4 mg /m^3 from March to April and minimum concentrations around 2 mg /m^3 in August. In general, simulated surface chlorophyll concentrations agree reasonably

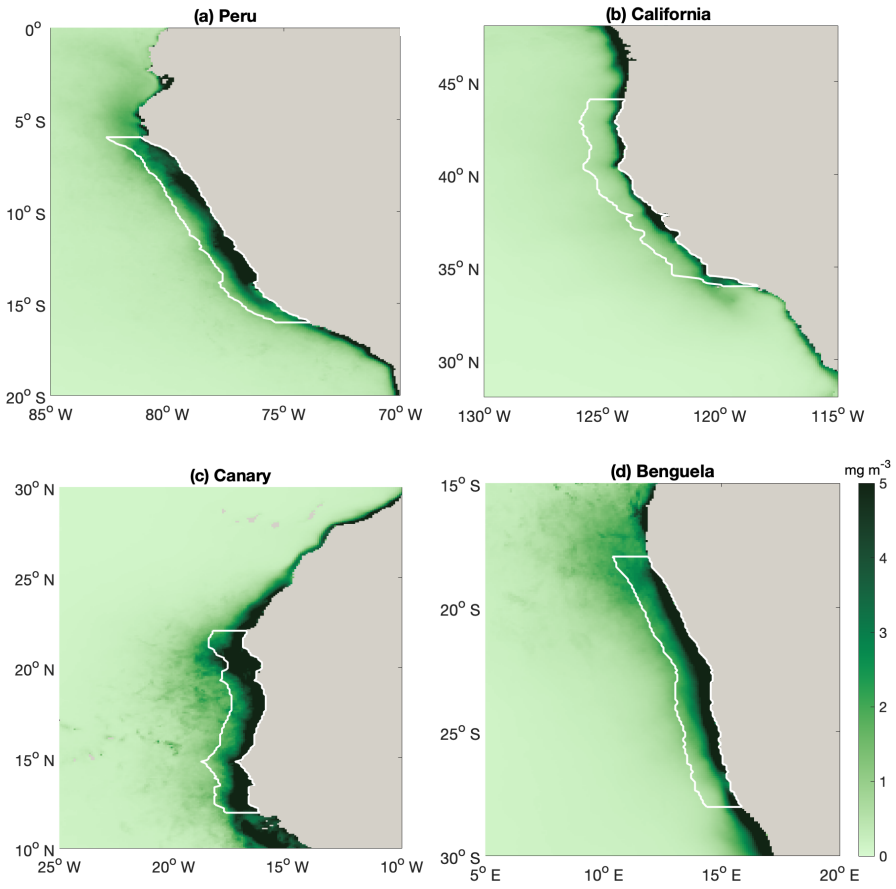

Figure A2. Map of annual mean surface chlorophyll ($mg\,chl\,m^{-3}$) with white lines highlight the regions that we average over in our analyses in Fig.2. Coastal EBUS regions picking here are the same as Chavez and Messié (2009)

well with satellite data.

B2 Surface nitrate concentration

The simulated surface nitrate distribution shows the same seasonality as observations from the World Ocean Atlas (WOA; Garcia et al., 2019) (Fig. B2). The simulated surface nitrate concentration in the coastal region is biased high compared to the WOA data. This may be partly due to the WOA data failing to capture high-nitrate concentrations due to coastal upwelling. This notion is supported by nitrate concentration data from a cruise in austral summer that show nitrate concentrations in the coastal region are high compared to the model data.

Table A1. Adjusted biological Parameters and range of published parameter values

Parameters	Symbols	Units	Value	Range
Max growth rate of P_L	a_{P_L}	d^{-1}	0.6	0.6[a]-3.0[b]
Mortality rate of P_L	μ_{P_L}	d^{-1}	0.15	0.027[c]-0.2[d]
Preference of Z_S for P_S	$e_{Z_S P_S}$	-	0.65	see references[e]
Preference of Z_S for P_L	$e_{Z_S P_L}$	-	0.35	see references[e]
Preference of Z_L for P_S	$e_{Z_L P_S}$	-	0.1	see references[f,g]
Preference of Z_L for P_L	$e_{Z_L P_L}$	-	0.4	see references[f,g]
Preference of Z_L for Z_S	$e_{Z_L Z_S}$	-	0.5	see references[f,g]
Excretion rate of Z_S	γ_{Z_S}	d^{-1}	0.1	0.03[h]-0.1[i]
Excretion rate of Z_L	γ_{Z_L}	d^{-1}	0.1	0.05[h]-0.1[i]
Mortality rate of Z_L	μ_{Z_L}	$\mathrm{mmol\,N\,m^{-3}\,d^{-1}}$	0.135	0.05[a]-0.25[j]

The values for diet preferences were picked based on a combination of calibrating the model against observations of plankton biomasses and observed qualitative diet preferences in the references.

[a] Gutknecht et al. (2013)

[b] Andersen et al. (1987)

[c] Koné et al. (2005)

[d] Taylor et al. (1991)

[e] Bohata (2016)

[f] Kleppel (1993)

[g] Schukat et al. (2014)

[h] Aumont (2005)

[i] Fennel et al. (2006)

[j] Lima and Doney (2004)

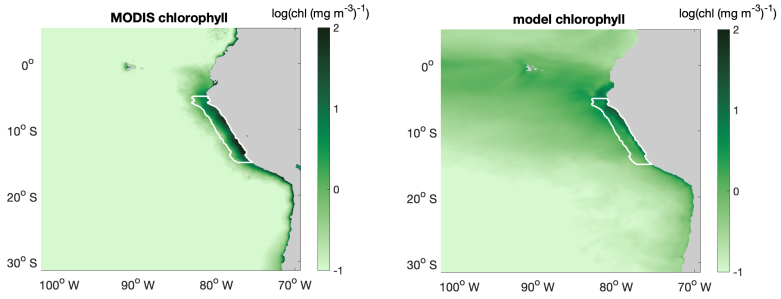

Figure B1. Annual mean surface chlorophyll concentration (in $\log(\mathrm{chl}\ (\mathrm{mg\,m^{-3}})^{-1})$) distribution of (a) MODIS and (b) CROCO-BioEBUS. White lines highlight the focus region.

B3 Mixed layer depth

We validate the simulated MLD against the gridded ARGO mixed layer dataset (Holte et al. (2017), http://mixedlayer.ucsd.edu/) both in terms of spatial pattern and seasonal variability within the research area (Fig. B3). The annually averaged spatial dis-

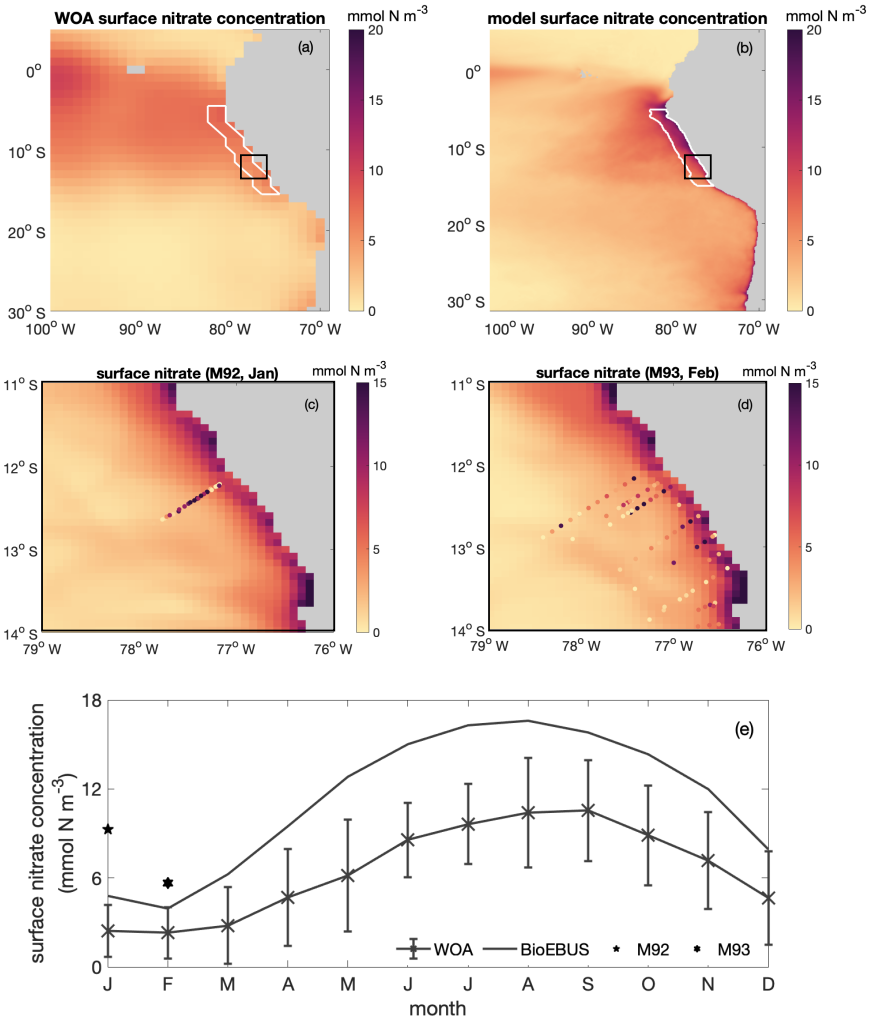

Figure B2. Spatial distribution of surface nitrate concentration based on (a) WOA and (b) CROCO-BioEBUS; (c) January and (d) February as simulated by CROCO-BioEBUS. Dots indicate measurements from the cruises M92 (January) and M93 (February); (e) seasonal cycle of surface nitrate concentration from WOA (cross), CROCO-BioEBUS (line) and cruises (pentagram, hexagram) within the focus region. White lines highlight the focus region. The black box indicates the maps of panel c-d.

tribution of MLD within the research area presents the same features as ARGO: shallower MLD in the coastal region (around 20 m) and deeper MLD in the offshore region (around 80 m). The simulated seasonal variability of MLD within the research region generally follows the seasonal trend of the Argo data. The water column within the research region is most stratified in February to March and most deeply mixed in August. Although simulated MLD in austral winter is somewhat deep, the simulated MLD are largely within the range of the ARGO data.

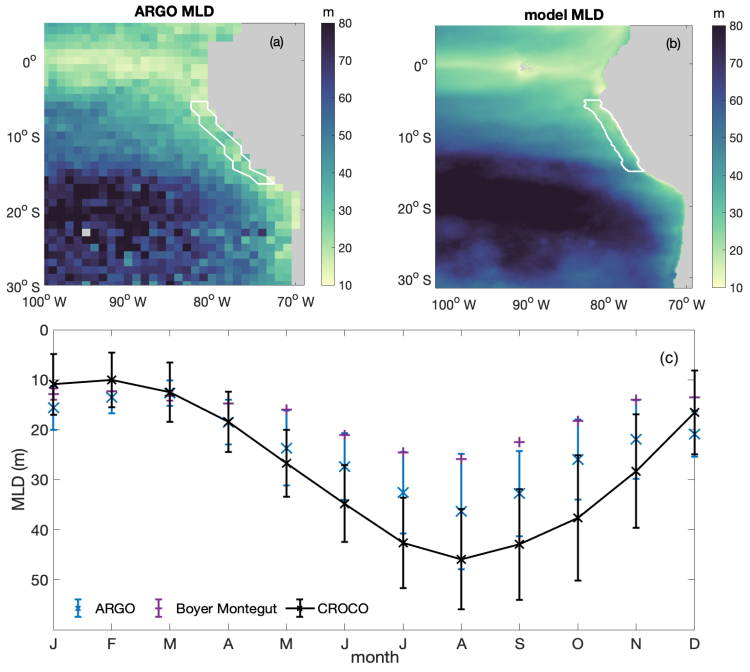

Figure B3. Annual average spatial distribution of mixed layer depth (MLD) from (a) ARGO and (b) CROCO-BioEBUS; (c) Seasonal variation of average mixed layer depth from ARGO (crosses, with lines indicating the standard deviation) and model simulation (line) within focus region. White lines highlight the focus region.

B4 Sea surface temperature

The simulated SST has been validated against monthly climatological MODIS data in terms of both spatial pattern and seasonal variability within the research area (Fig. B4). The annually averaged spatial distribution of SST is well simulated by the model. The model successfully captures the cold coastal upwelled water as well as slightly warmer water masses further offshore. The simulated SST seasonality within the research region generally follows the seasonal trend of the observations, with a cool bias of less than 1^oC. The surface waters within the research region are warmest in February to March matching the modelled/observed shallowest mixed layers and coldest from August to October. In general, the simulated SST matches the observations well both in terms of spatial pattern and seasonal variation.

B5 Mesozooplankton distribution

In addition, we calibrated zooplankton in the BioEBUS model against observational estimates (Fig. B5). It is something that is often omitted, despite the central role of zooplankton parameterisations on plankton dynamics (Anderson et al., 2010; Prowe et al., 2012) . While the observations show a large spread, the simulated large-scale spatial distribution of mesozooplankton generally follows the observed pattern, with high mesozooplankton biomass in the upwelling region and low biomass further offshore.

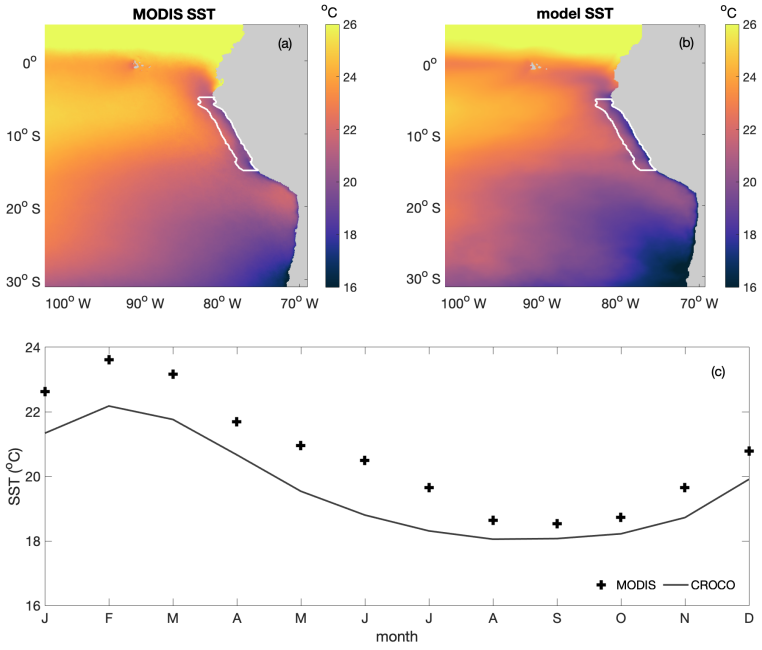

Figure B4. Annual average spatial distribution of sea surface temperature (SST, in ^oC) from (a) MODIS and (b) CROCO-BioEBUS; (c) Seasonal variation of average sea surface temperature (SST) from MODIS (cross) and model simulation (line) within focus region. White lines highlight the focus region.

The model simulates a stripe of low zooplankton biomass concentrations in the focus region near the coast (due to offshore advection combined with slow mesozooplankton growth) that is difficult to assess, as observations near the coast are sparse. Though, the feature is apparent to some extent in the observations in the southern focus region.

Appendix C: Additional Figures

The whole time series of temperature and nitrate concentration at 10 m and ~~1000~~ 100 m are shown in Fig. C1a-b. Surface fields are spun up after one year while ~~deepwater takes~~ water at 100 m takes 3-10 years longer to reach a steady state. In the meanwhile, mixed layer and surface layer chlorophyll are also spun up after one year (Fig. C1c-d).

~~Detailed seasonal cycles of phytoplankton budgets integrated over MLD is shown in Fig. C2, including primary production (pp), consumptive mortality (graz), natural mortality (mort), exudation (exu), sinking (sink), mixing (mix), advection (adv) and entrainment (entr). Further, seasonalities of net biological (bio) and physical (phy) fluxes along with MLD-integrated phytoplankton biomass change (ΔB) is also shown in the figure.~~

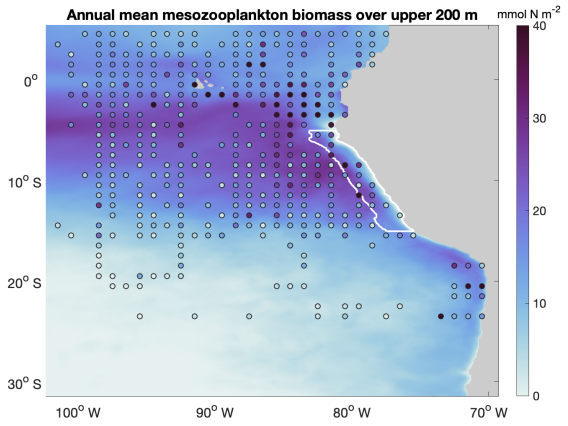

Figure B5. Annual average spatial distribution of integrated mesozooplankton biomass over upper 200 m (in $mmolNm^{-2}$). Dots indicate mesozooplankton data from observations (Moriarty and O'Brien, 2013, https://doi.org/10.5194/essd-5-45-2013). White lines highlight the focus region.

~~Seasonal cycles of phytoplankton source and sink processes integrated over the mixed layer, along with the net biological fluxes (dotted line) and the net physical fluxes (dashed line), and the tendency (change) of phytoplankton biomass (solid line) integrated over the mixed layer.~~

Apart from above mentioned mixed layer depth and upwelling intensity, short-wave surface radiation and surface net heat flux are of second-order importance to light- and temperature-related variance during the decline phase respectively (Fig.C2).

Phytoplankton net advection flux over the mixed layer closely follows the upwelling intensity during the decline phase (Fig.C3, $R^2 = 0.81$). When the mixed layer depth is relatively shallow, the correlation between upwelling intensity and phytoplankton convergence of advection over the mixed layer is insignificant.

~~We define export as the organic material sinking below the euphotic layer and export efficiency as the ratio of primary production over export (Murray et al., 1996). The efficiency of export depends on the composition of particle organic matter with different sinking speed and its remineralization rate. Within the model, export efficiency is positively correlated with net primary production (Fig. C5) which is opposite to what is found in the California system.~~

~~Correlation of export efficiency (defined as ratio of primary production over export below the euphotic layer) with net primary production (NPP). Colors indicate the time of the year.~~

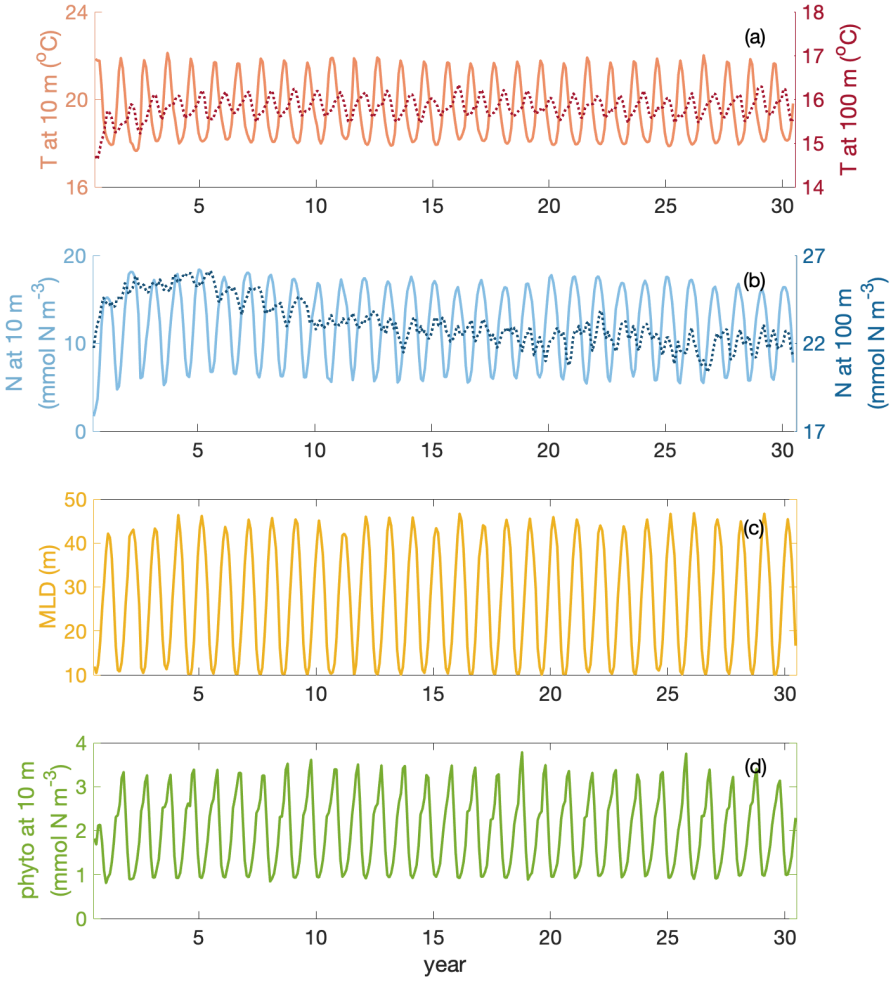

Figure C1. Time series of temperature T (at 10 m & ~~1000~~100 m depth), nitrate N (at 10 m & ~~1000~~100 m depth), mixed layer depth MLD and phytoplankton phyto (at 10 m) over 30 years of simulation in the focus region.

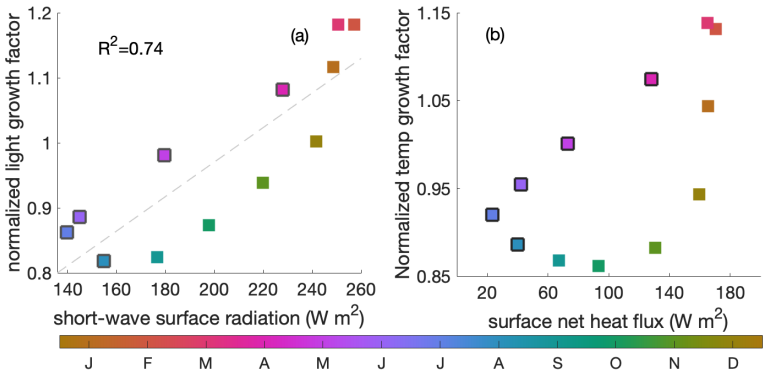

Figure C2. (a) Correlation between surface short-wave radiation (Wm^{-2}) and the averaged light-related growth factor within mixed layer; (b) Correlation between the surface heat forcing (in $^{\circ}\mathrm{Cd}^{-1}$) and averaged temperature-related growth factor within mixed layer. ~~Color~~ Colour indicates the time of the year and black edges the decline phase.

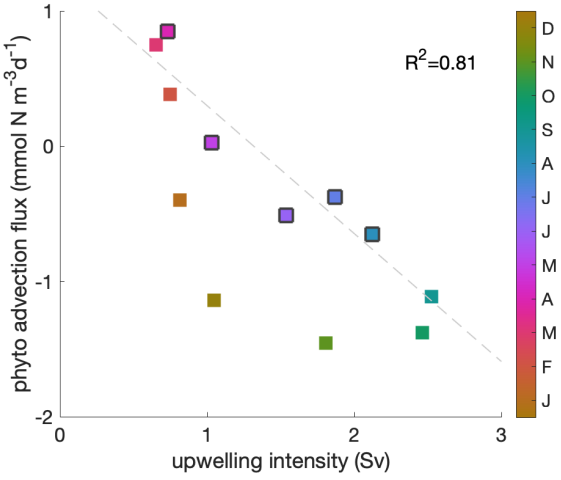

Figure C3. Correlation between upwelling intensity and phytoplankton convergence of advection over the mixed layer. A negative convergence equals a divergence of phytoplankton biomass due to the combined effect of upwelling and lateral transports. Color indicates the time of the year and black edges the decline phase. The correlation coefficient (R^2=0.81) is shown for the decline phase.

Author contributions. IF and AO designed the study. TX and YSJ carried out the simulations. TX, IF and FP conducted the analysis. All authors discussed the results and wrote the manuscript.

Competing interests. The authors declare that they have no conflict of interest.

Acknowledgements. This work is financially supported by the China Scholarship Council (TX, grant no.201808460055). Further support for this work was provided by the BMBF funded projects Coastal Upwelling System in a Changing Ocean CUSCO (IF, AO) and Humboldt Tipping (YJ).

References

Albert, A., Echevin, V., Lévy, M., and Aumont, O.: Impact of nearshore wind stress curl on coastal circulation and primary productivity in the Peru upwelling system, Journal of Geophysical Research: Oceans, 115, 2010.

Andersen, V., Nival, P., and Harris, R. P.: Modelling of a planktonic ecosystem in an enclosed water column, Journal of the Marine Biological Association of the United Kingdom, 67, 407–430, 1987.

Anderson, T. R., Gentleman, W. C., and Sinha, B.: Influence of grazing formulations on the emergent properties of a complex ecosystem model in a global ocean general circulation model, Progress in Oceanography, 87, 201–213, 2010.

Aumont, O.: PISCES biogeochemical model, Unpublished report, 2005.

Bakun, A.: Coastal upwelling indices, west coast of North America, 1946-71, 1973.

Bakun, A.: Global climate change and intensification of coastal ocean upwelling, Science, 247, 198–201, 1990.

Bakun, A., Field, D. B., Redondo-Rodriguez, A., and Weeks, S. J.: Greenhouse gas, upwelling-favorable winds, and the future of coastal ocean upwelling ecosystems, Global Change Biology, 16, 1213–1228, 2010.

Behrenfeld, M. J.: Climate-mediated dance of the plankton, Nature Climate Change, 4, 880–887, 2014.

Bohata, K.: Microzooplankton of the northern Benguela Upwelling System, PhD thesis, 2016.

Bruland, K. W., Rue, E. L., Smith, G. J., and DiTullio, G. R.: Iron, macronutrients and diatom blooms in the Peru upwelling regime: brown and blue waters of Peru, Marine Chemistry, 93, 81–103, 2005.

Calienes, R., Guillén, O., Lostaunau, N., et al.: Variabilidad espacio-temporal de clorofila, producción primaria y nutrientes frente a la costa peruana, Boletin Instituto del Mar del Peru, 10, 1–44, 1985.

Carton, J. A. and Giese, B. S.: A reanalysis of ocean climate using Simple Ocean Data Assimilation (SODA), Monthly Weather Review, 136, 2999–3017, 2008.

Chavez, F. P.: A comparison of ship and satellite chlorophyll from California and Peru, Journal of Geophysical Research: Oceans, 100, 24 855–24 862, 1995.

Chavez, F. P. and Messié, M.: A comparison of eastern boundary upwelling ecosystems, Progress in Oceanography, 83, 80–96, 2009.

Chavez, F. P., Bertrand, A., Guevara-Carrasco, R., Soler, P., and Csirke, J.: The northern Humboldt Current System: Brief history, present status and a view towards the future, Progress in Oceanography, 79, 95–105, 2008.

Debreu, L., Marchesiello, P., Penven, P., and Cambon, G.: Two-way nesting in split-explicit ocean models: Algorithms, implementation and validation, Ocean Modelling, 49, 1–21, 2012.

Ducklow, H. W., Steinberg, D. K., and Buesseler, K. O.: Upper ocean carbon export and the biological pump, OCEANOGRAPHY-WASHINGTON DC-OCEANOGRAPHY SOCIETY-, 14, 50–58, 2001.

Echevin, V., Aumont, O., Ledesma, J., and Flores, G.: The seasonal cycle of surface chlorophyll in the Peruvian upwelling system: A modelling study, Progress in Oceanography, 79, 167–176, 2008.

Echevin, V., Gévaudan, M., Espinoza-Morriberón, D., Tam, J., Aumont, O., Gutierrez, D., and Colas, F.: Physical and biogeochemical impacts of RCP8. 5 scenario in the Peru upwelling system, Biogeosciences, 17, 3317–3341, 2020.

Fennel, K., Wilkin, J., Levin, J., Moisan, J., O'Reilly, J., and Haidvogel, D.: Nitrogen cycling in the Middle Atlantic Bight: Results from a three-dimensional model and implications for the North Atlantic nitrogen budget, Global Biogeochemical Cycles, 20, 2006.

Friederich, G. E., Ledesma, J., Ulloa, O., and Chavez, F. P.: Air–sea carbon dioxide fluxes in the coastal southeastern tropical Pacific, Progress in Oceanography, 79, 156–166, 2008.

Fuenzalida, R., Schneider, W., Garcés-Vargas, J., Bravo, L., and Lange, C.: Vertical and horizontal extension of the oxygen minimum zone in the eastern South Pacific Ocean, Deep Sea Research Part II: Topical Studies in Oceanography, 56, 992–1003, 2009.

Fung, I. Y., Meyn, S. K., Tegen, I., Doney, S. C., John, J. G., and Bishop, J. K.: Iron supply and demand in the upper ocean, Global Biogeochemical Cycles, 14, 281–295, 2000.

Garcia, H., Weathers, K., Paver, C., Smolyar, I., Boyer, T., Locarnini, M., Zweng, M., Mishonov, A., Baranova, O., Seidov, D., et al.: World Ocean Atlas 2018. Vol. 4: Dissolved Inorganic Nutrients (phosphate, nitrate and nitrate+ nitrite, silicate), 2019.

Getzlaff, J., Dietze, H., and Oschlies, A.: Simulated effects of southern hemispheric wind changes on the Pacific oxygen minimum zone, Geophysical Research Letters, 43, 728–734, 2016.

Grémillet, D., Lewis, S., Drapeau, L., van Der Lingen, C. D., Huggett, J. A., Coetzee, J. C., Verheye, H. M., Daunt, F., Wanless, S., and Ryan, P. G.: Spatial match–mismatch in the Benguela upwelling zone: should we expect chlorophyll and sea-surface temperature to predict marine predator distributions?, Journal of Applied Ecology, 45, 610–621, 2008.

Guillen, O. and Calienes, R.: Upwelling off chimbote, Coastal upwelling, 1, 312–326, 1981.

Gutiérrez, D., Bouloubassi, I., Sifeddine, A., Purca, S., Goubanova, K., Graco, M., Field, D., Méjanelle, L., Velazco, F., Lorre, A., et al.: Coastal cooling and increased productivity in the main upwelling zone off Peru since the mid-twentieth century, Geophysical Research Letters, 38, 2011.

Gutknecht, E., Dadou, I., Le Vu, B., Cambon, G., Sudre, J., Garçon, V., Machu, E., Rixen, T., Kock, A., Flohr, A., et al.: Coupled physical/biogeochemical modeling including O2-dependent processes in the Eastern Boundary Upwelling Systems: application in the Benguela, Biogeosciences, 10, 3559–3591, 2013.

Henson, S., Le Moigne, F., and Giering, S.: Drivers of carbon export efficiency in the global ocean, Global biogeochemical cycles, 33, 891–903, 2019.

Holte, J., Talley, L. D., Gilson, J., and Roemmich, D.: An Argo mixed layer climatology and database, Geophysical Research Letters, 44, 5618–5626, 2017.

José, Y. S., Dietze, H., and Oschlies, A.: Linking diverse nutrient patterns to different water masses within anticyclonic eddies in the upwelling system off Peru, Biogeosciences, 14, 1349–1364, 2017.

Kelly, T. B., Goericke, R., Kahru, M., Song, H., and Stukel, M. R.: CCE II: Spatial and interannual variability in export efficiency and the biological pump in an eastern boundary current upwelling system with substantial lateral advection, Deep Sea Research Part I: Oceanographic Research Papers, 140, 14–25, 2018.

Kleppel, G.: On the diets of calanoid copepods, Marine Ecology-Progress Series, 99, 183–183, 1993.

Koné, n. V., Machu, E., Penven, P., Andersen, V., Garçon, V., Fréon, P., and Demarcq, H.: Modeling the primary and secondary productions of the southern Benguela upwelling system: A comparative study through two biogeochemical models, Global Biogeochemical Cycles, 19, 2005.

Lachkar, Z. and Gruber, N.: What controls biological production in coastal upwelling systems? Insights from a comparative modeling study, Biogeosciences, 8, 2961–2976, 2011.

Lima, I. D. and Doney, S. C.: A three-dimensional, multinutrient, and size-structured ecosystem model for the North Atlantic, Global Biogeochemical Cycles, 18, 2004.

Liu, W. T., Tang, W., and Polito, P. S.: NASA scatterometer provides global ocean-surface wind fields with more structures than numerical weather prediction, Geophysical Research Letters, 25, 761–764, 1998.

Messié, M. and Chavez, F. P.: Seasonal regulation of primary production in eastern boundary upwelling systems, Progress in Oceanography, 134, 1–18, 2015.

Messié, M., Ledesma, J., Kolber, D. D., Michisaki, R. P., Foley, D. G., and Chavez, F. P.: Potential new production estimates in four eastern boundary upwelling ecosystems, Progress in Oceanography, 83, 151–158, 2009.

Montes, I., Dewitte, B., Gutknecht, E., Paulmier, A., Dadou, I., Oschlies, A., and Garçon, V.: High-resolution modeling of the Eastern Tropical Pacific oxygen minimum zone: Sensitivity to the tropical oceanic circulation, Journal of Geophysical Research: Oceans, 119, 5515–5532, 2014.

Moriarty, R. and O'Brien, T.: Distribution of mesozooplankton biomass in the global ocean, Earth System Science Data, 5, 45–55, 2013.

Murray, J. W., Young, J., Newton, J., Dunne, J., Chapin, T., Paul, B., and McCarthy, J. J.: Export flux of particulate organic carbon from the central equatorial Pacific determined using a combined drifting trap-234Th approach, Deep Sea Research Part II: Topical Studies in Oceanography, 43, 1095–1132, 1996.

O'Reilly, J. E., Maritorena, S., Mitchell, B. G., Siegel, D. A., Carder, K. L., Garver, S. A., Kahru, M., and McClain, C.: Ocean color chlorophyll algorithms for SeaWiFS, Journal of Geophysical Research: Oceans, 103, 24 937–24 953, 1998.

Pauly, D., Christensen, V., Dalsgaard, J., Froese, R., and Torres, F.: Fishing down marine food webs, Science, 279, 860–863, 1998.

Pennington, J. T., Mahoney, K. L., Kuwahara, V. S., Kolber, D. D., Calienes, R., and Chavez, F. P.: Primary production in the eastern tropical Pacific: A review, Progress in oceanography, 69, 285–317, 2006.

Prowe, A. F., Pahlow, M., Dutkiewicz, S., Follows, M., and Oschlies, A.: Top-down control of marine phytoplankton diversity in a global ecosystem model, Progress in Oceanography, 101, 1–13, 2012.

Ridgway, K., Dunn, J., and Wilkin, J.: Ocean interpolation by four-dimensional weighted least squares—Application to the waters around Australasia, Journal of atmospheric and oceanic technology, 19, 1357–1375, 2002.

Schukat, A., Auel, H., Teuber, L., Lahajnar, N., and Hagen, W.: Complex trophic interactions of calanoid copepods in the Benguela upwelling system, Journal of Sea Research, 85, 186–196, 2014.

Shchepetkin, A. F. and McWilliams, J. C.: The regional oceanic modeling system (ROMS): a split-explicit, free-surface, topography-following-coordinate oceanic model, Ocean modelling, 9, 347–404, 2005.

Steinberg, D. K. and Landry, M. R.: Zooplankton and the ocean carbon cycle, Annual review of marine science, 9, 413–444, 2017.

Stramma, L., Schmidtko, S., Levin, L. A., and Johnson, G. C.: Ocean oxygen minima expansions and their biological impacts, Deep Sea Research Part I: Oceanographic Research Papers, 57, 587–595, 2010.

Stukel, M. R., Ohman, M. D., Benitez-Nelson, C. R., and Landry, M. R.: Contributions of mesozooplankton to vertical carbon export in a coastal upwelling system, Marine Ecology Progress Series, 491, 47–65, 2013.

Sunda, W. G. and Huntsman, S. A.: Interrelated influence of iron, light and cell size on marine phytoplankton growth, Nature, 390, 389–392, 1997.

Suttle, C. A.: Viruses in the sea, Nature, 437, 356–361, 2005.

Taylor, A., Watson, A., Ainsworth, M., Robertson, J., and Turner, D.: A modelling investigation of the role of phytoplankton in the balance of carbon at the surface of the North Atlantic, Global Biogeochemical Cycles, 5, 151–171, 1991.

Tedesco, P., Gula, J., Ménesguen, C., Penven, P., and Krug, M.: Generation of submesoscale frontal eddies in the Agulhas Current, Journal of Geophysical Research: Oceans, 124, 7606–7625, 2019.

Thomas, A., Carr, M.-E., and Strub, P. T.: Chlorophyll variability in eastern boundary currents, Geophysical Research Letters, 28, 3421–3424, 2001.

Turner, J. T.: Zooplankton fecal pellets, marine snow, phytodetritus and the ocean's biological pump, Progress in Oceanography, 130, 205–248, 2015.

Worley, S. J., Woodruff, S. D., Reynolds, R. W., Lubker, S. J., and Lott, N.: ICOADS release 2.1 data and products, International Journal of Climatology: A Journal of the Royal Meteorological Society, 25, 823–842, 2005.